



1 **AERO-MAP: A data compilation and modelling approach to**

2 **understand spatial variability in fine and coarse mode aerosol**

3 **composition**

4 Natalie M. Mahowald¹, Longlei Li¹, Julius Vira², Marje Prank², Douglas S. Hamilton³, Hitoshi Matsui⁴, Ron L. Miller⁵,
5 Louis Lu¹, Ezgi Akyuz⁶, Daphne Meidan¹, Peter Hess⁷, Heikki Lihavainen⁸, Christine Wiedinmyer⁹, Jenny Hand¹⁰, Maria
6 Grazia Alaimo¹¹, Célia Alves¹², Andres Alastuey¹³, Paulo Artaxo¹⁴, Africa Barreto¹⁵, Francisco Barraza¹⁶, Silvia Becagli¹⁷,
7 Giulia Calzolai¹⁷, Shankararaman Chellam¹⁸, Ying Chen¹⁹, Patrick Chuang²⁰, David D. Cohen²¹, Cristina Colombi²²,
8 Evangelia Diapouli²³, Gaetano Dongarra¹¹, Konstantinos Eleftheriadis²³, Johann Engelbrecht²⁴, Corinne Galy-Lacaux²⁵,
9 Cassandra Gaston²⁶, Dario Gomez²⁷, Yenny González Ramos^{28,15}, Roy M. Harrison²⁹, Chris Heyes³⁰, Barak Herut^{31,32}, Philip
10 Hopke^{33,34}, Christoph Hüglin³⁵, Maria Kanakidou^{36,37,38}, Zsofia Kertesz³⁹, Zbigniew Klimont³⁰, Katriina Kyllonen², Fabrice
11 Lambert^{40,41}, Xiaohong Liu⁴², Remi Losno⁴³, Franco Lucarelli¹⁷, Willy Maenhaut⁴⁴, Beatrice Marticorena⁴⁵, Randall V.
12 Martin⁴⁶, Nikolaos Mihalopoulos^{35,47}, Yasser Morera-Gomez⁴⁸, Adina Paytan⁴⁹, Joseph Prospero²⁵, Sergio Rodríguez^{50,15},
13 Patricia Smichowski²⁷, Daniela Varrica¹¹, Brenna Walsh⁴⁶, Crystal Weagle⁴⁶, Xi Zhao⁴²

14 ¹Department of Earth and Atmospheric Sciences, Cornell University, Ithaca, NY, 14853, USA

15 ² Finnish Meteorological Institute, Helsinki, Finland

16 ³ Department of Marine, Earth and Atmospheric Sciences, North Carolina State, Raleigh, NC, USA

17 ⁴ Graduate School of Environmental Studies, Nagoya University, Nagoya, Japan 464-8601

18 ⁵ National Aeronautics and Space Administration, Goddard Institute for Space Studies, Columbia University, NY, NY 10025

19 ⁶ Eurasia Institute of Earth Sciences, Istanbul Technical University, 34467 Istanbul, Turkey

20 ⁷ Department of Biological and Environmental Engineering, Cornell University, Ithaca NY, USA

21 ⁸ SIOS Knowledge Centre, Postboks 156, 9171 Longyearbyen, Norway

22 ⁹ Cooperative Institute for Research in Environmental Sciences at the University of Colorado Boulder, Boulder, CO, USA

23 ¹⁰ Cooperative Institute for Research in the Atmosphere, Colorado State University, Fort Collins, CO, USA,

24 ¹¹ Dip. Scienze della Terra e del Mare, University of Palermo, Italy

25 ¹² Centre for Environmental and Marine Studies (CESAM), Department of Environment, University of Aveiro, 3810-193, Aveiro, Portugal

26 ¹³ Institute of Environmental Assessment and Water Research (IDAEA-CSIC), 08034, Barcelona, Spain

27 ¹⁴ Instituto de Fisica, Universidade de Sao Paulo, 05508-090, Sao Paulo, SP, Brazil

28 ¹⁵ Izaña Atmospheric Research Center (IARC), Agencia Estatal de Meteorología (AEMET), Santa Cruz de Tenerife, Spain



- 30 ¹⁶ Saw Science, Invercargill, New Zealand
- 31 ¹⁷ Department of Physics and Astronomy, Universita di Firenze and INFN-Firenze, 50019 Sesto Fiorentino, Italy
- 32 ¹⁸ Department of Civil & Environmental Engineering, Texas A&M University, College Station, TX 77843-3136, USA
- 33 ¹⁹ Dept. Environ. Sci. Engr. Fudan University Jiangwan Campus 2005 Songhu Road, Shanghai, China
- 34 ²⁰ Earth & Planetary Sciences Department, Institute of Marine Sciences, University of California, Santa Cruz, CA, 95064 ,
35 USA.
- 36 ²¹ Centre for Accelerator Science, Australian Nuclear Science and Technology Organisation, New Illawarra Rd, Lucas
37 Heights, NSW, Australia
- 38 ²² Environmental Monitoring Sector, Arpa Lombardia, Via Rosellini 17, 20124 Milan, Italy
- 39 ²³ Environmental Radioactivity & Aerosol Technology for Atmospheric & Climate impact Lab, INRaSTES, N.C.S.R.
40 Demokritos, 15341 Ag. Paraskevi, Attiki, Greece
- 41 ²⁴ Desert Research Institute (DRI), 2215 Raggio Parkway, Reno, Nevada 89512-1095
- 42 ²⁵ Laboratoire d Aerologie, Universite de Toulouse, CNRS, Observatoire Midi Pyrenees, Toulouse, France
- 43 ²⁶ Rosenstiel School of Marine and Atmospheric Science, University of Miami, Miami, FL, 33149, US
- 44 ²⁷ Comision Nacional de Energia Atomica, Gerencia Química, Av. Gral Paz 1499, B1650KNA, San Martin, Buenos Aires,
45 Argentina
- 46 ²⁸ Scientific Department, CIMEL, Paris, France.
- 47 ²⁹ School of Geography, Earth and Environmental Sciences, University of Birmingham, Edgbaston, Birmingham B15 2TT,
48 United Kingdom
- 49 ³⁰ Energy, Climate and Environment Program, International Institute for Applied Systems Analysis, 2361 Laxenburg,
50 Austria
- 51 ³¹ Israel Oceanographic & Limnological Research, Tel Shikmona, Haifa, 31080, Israel
- 52 ³² University of Haifa, Haifa, 3103301, Israel
- 53 ³³ Clarkson University, Potsdam, NY, USA,
- 54 ³⁴ Department of Public Health Sciences, University of Rochester School of Medicine and Dentistry, Rochester, NY, USA,
- 55 ³⁵ Swiss Federal Laboratories for Materials Science and Technology(EMPA), CH-8600 Duebendorf, Switzerland
- 56 ³⁶ Environmental Chemical Processes Laboratory (ECPL), Department of Chemistry, University of Crete, Heraklion, Greece.
- 57 ³⁷ Center of Studies of Air quality and Climate Change, Institute for Chemical Engineering Sciences, Foundation for
58 Research and Technology Hellas, Patras, Greece.
- 59 ³⁸ Excellence Chair, Institute of Environmental Physics, University of Bremen, Bremen, Germany
- 60 ³⁹ HUN-REN Institute for Nuclear Research (ATOMKI), Debrecen, Hungary
- 61 ⁴⁰ Geography Institute, Pontificia Universidad Catolica de Chile, Santiago, 7820436, Chile
- 62 ⁴¹ Center for Climate and Resilience Research, Santiago, Chile
- 63 ⁴² Department of Atmospheric Sciences, Texas A&M University, College Station, TX 77843
- 64 ⁴³ Institut de Physique du Globe de Paris, Universite de Paris, Paris, France
- 65 ⁴⁴ Department of Chemistry, Ghent University, Gent, Belgium
- 66 ⁴⁵ Laboratoire Interuniversitaire des Systemes Atmospheriques (LISA), Universit es Paris Est-Paris Diderot-Paris 7, UMR
67 CNRS 7583, Cr eteil, France
- 68 ⁴⁶ Energy, Environmental and Chemical Engineering, Washington University, St. Louis, MO, USA.
- 69 ⁴⁷ Institute for Environmental Research and Sustainable Development, National Observatory of Athens, Pendeli, Greece
- 70 ⁴⁸ Universidad de Navarra, Instituto de Biodiversidad y Medioambiente BIOMA, Irunlarrea 1, 31008, Pamplona, Espa a



71 ⁴⁹ Earth and Planetary Science, University of California, Santa Cruz, CA, USA

72 ⁵⁰ Consejo Superior de Investigaciones Científicas, IPNA CSIC, Tenerife, Canary Islands, Spain.

73
74
75 *Correspondence to:* Natalie M. Mahowald (mahowald@cornell.edu)

76 **Abstract.** Aerosol particles are an important part of the Earth system, but their concentrations are spatially and temporally
77 heterogeneous, as well as variable in size and composition. Particles can interact with incoming solar radiation and outgoing
78 long wave radiation, change cloud properties, affect photochemistry, impact surface air quality, change the surface albedo of
79 snow and ice, and modulate carbon dioxide uptake by the land and ocean. High particulate matter concentrations at the
80 surface represent an important public health hazard. There are substantial datasets describing aerosol particles in the
81 literature or in public health databases, but they have not been compiled for easy use by the climate and air quality modelling
82 community. Here we present a new compilation of PM_{2.5} and PM₁₀ aerosol observations, focusing on the spatial variability
83 across different observational stations, including composition, and demonstrate a method for comparing the datasets to
84 model output. Overall, most of the planet or even the land fraction does not have sufficient observations of surface
85 concentrations, and especially particle composition to understand the current distribution of particles. Most climate models
86 exclude 10-30% of the aerosol particles in both PM_{2.5} and PM₁₀ size fractions across large swaths of the globe in their current
87 configurations, with ammonium nitrate and agricultural dust aerosol being the most important omitted aerosol types.

88

89 1 Introduction

90 Intergovernmental Panel on Climate Change (IPCC) reports and studies have highlighted the role of uncertainties in human-
91 induced changes to aerosol concentration and composition in the atmosphere in limiting our ability to project future climate
92 (IPCC, 2021; Gulev et al., 2021; Szopa et al., 2021). Aerosol particles are also a major contributor to air quality problems,
93 which reduce life expectancy and quality of life (Burnett et al., 2018). Aerosol particles are suspended liquids or solids in the
94 atmosphere originating from diverse sources and composed of a wide variety of chemicals (e.g., sea salts, dust, sulfate,
95 nitrate, black carbon, organic carbon). Particles interact with incoming solar radiation, outgoing long wave radiation, change
96 cloud properties and lifetimes, and modify atmospheric photochemistry (Mahowald et al., 2011; Kanakidou et al., 2018;
97 Bellouin et al., 2020). Once deposited on the surface, they can modify land and ocean biogeochemistry, as well as the
98 albedo of snow and ice surfaces (Mahowald et al., 2017; Hansen and Nazarenko, 2004; Skiles et al., 2018). New satellite
99 remote sensing measurements provide important information about temporal and spatial distribution of aerosol particles, but
100 challenges remain in quantifying the size and chemical composition of aerosol (Kahn et al., 2005; Tanré et al., 1997; Remer
101 et al., 2005). In addition, the AERONET surface remote sensing network provides some information about loading, size and



102 absorbing aerosol properties related to composition (Holben et al., 1991; Dubovik et al., 2002; Schuster et al., 2016;
103 Gonçalves Ageitos et al., 2023; Obiso et al., 2023). Both the magnitude of the effects, and sometimes the sign of the aerosol
104 effects on climate are dependent on the composition and size of particles (Mahowald et al., 2011, 2014a; Bond et al., 2013;
105 IPCC, 2021). In addition, one cannot understand the impact of humans on aerosol particles without understanding the
106 sources of particles, which determines their chemical composition. Obtaining information about the composition and size of
107 particles in many cases requires in situ observations, which are limited in space and time (Hand et al., 2017; Philip et al.,
108 2017; Yang et al., 2018; Collaud Coen et al., 2020).

109 The climate and aerosol modelling community, especially under the auspices of AEROCOM, has compiled datasets and
110 organized comparison projects that have provided substantial information to improve aerosol models (Huneeus et al., 2011;
111 Textor and others, 2006; Dentener et al., 2006; Schulz et al., 2006; Gliß et al., 2021) or knowledge of the aerosol properties
112 like cloud condensation nuclei (Laj et al., 2020; Fanourgakis et al., 2019). However, most of these comparisons include data
113 only from North America and Europe (e.g., Szopa et al., 2021). In addition, previous compilation studies have focused
114 primarily on understanding fine aerosol particles (here defined as particle with a diameter less than 2.5 μm) and improving
115 model simulation of these particles, because of their importance for air quality, cloud interactions and short-wave forcing
116 (Collaud Coen et al., 2020; Bellouin et al., 2020; Fanourgakis et al., 2019). Coarse mode particles (defined as those particles
117 with a diameter larger than 2.5 μm) are important for long wave radiation interactions, cloud seeding and for
118 biogeochemistry, but these interactions have received less attention (Jensen and Lee, 2008; Mahowald et al., 2011; Karydis
119 et al., 2017; Chatziparaschos et al., 2023). In contrast to the many fine aerosol compilations and comparisons (usually
120 considering particles with diameter less than 2.5 μm or PM_{2.5}), there are fewer studies focusing on aerosol compilations for
121 both fine and coarse particles, and their comparison to models (Kok et al., 2014b; Albani et al., 2014b; Huneeus et al., 2011;
122 Gliß et al., 2021; Kok et al., 2021). Nonetheless, there are many observations of the coarse particle mass included in the
123 particles with diameter less than 10 μm (PM₁₀) (e.g., Hand et al., 2017), and most climate models include these particles
124 (e.g., Huneeus et al., 2011). Compilations of in situ data are available for dust and iron particles (Kok et al., 2014b; Albani et
125 al., 2014b; Mahowald et al., 2009) and for sea salts (Gong et al., 1997). Other studies have focused on the important topics
126 of wet deposition (Vet et al., 2014) or trends in aerosol properties (e.g., AOD, surface PM) (Mortier et al., 2020; Aas et al.,
127 2019). Observations of PM₁₀ or coarse and fine particles are available for many regions and individual sites (e.g., Malm et
128 al., 2007; Hand et al., 2019; Maenhaut and Cafmeyer, 1998; Artaxo and Maenhaut, 1990; McNeill et al., 2020) but have not
129 previously been compiled into one database. Aerosol modelers need as much information as possible about the composition
130 of the particles. Thus, there is a need to compile both PM_{2.5} and PM₁₀ in situ concentration data into one database to make it
131 easy for modellers to compare model results with observations. One goal the aerosol community should work towards is
132 making aerosol measurement datasets publicly available, while acknowledging the principal investigators who produced
133 these datasets, which we hope this paper serves as a step towards achieving.



134 The current generation of Earth system models used for the IPCC simulations tends to include the dominant aerosol
135 particles (desert dust, sea spray, black carbon (BC), organic matter (OM) and sulfate) but not all particles. For example,
136 some Earth system models ignore ammonium nitrate particles although these are known to be important for climate and
137 biogeochemistry, and are impacted by human activities (Paulot et al., 2016; Adams et al., 1999; Thornhill et al., 2020). In
138 addition, some models focus only on fine mode OM and BC particles, although there is evidence for coarse mode particles of
139 both carbonaceous particles (Graham et al., 2003; Mahowald et al., 2005). Agricultural or land use sources of dust are not
140 included in most models, although they could represent 25% of the anthropogenic sources (Ginoux et al., 2012), and
141 significantly impact transported transhemispheric aerosol composition (García et al., 2017). In addition, fugitive, combustion
142 and industrial dust emissions have traditionally been ignored as well, although emission datasets are available (Philip et al.,
143 2017). In this study we use available observations to constrain a model estimate of the total PM₁₀ and PM_{2.5}, and deduce the
144 importance of these often-neglected aerosol particles. We propose a method for comparing particles that are not directly
145 measured (dust or sea salts) using their elemental composition. Note that we exclude super coarse (>PM₁₀) particles here
146 because of the lack of available data, although studies have suggested their importance for climate interactions (e.g., Adebyi
147 et al., 2023).

148 Aerosols are highly heterogeneous in space and time: here we focus on characterizing in observations and models the
149 spatial variability of the surface concentrations, as it is arguably the largest, spanning 4-5 orders of magnitude (e.g.,
150 Mahowald et al., 2011; Section 3.2). Spatial variability in surface concentrations is one of the least well known, for example
151 in the many unmonitored regions of the globe (e.g., Szopa et al., 2021). Understanding spatial variability in aerosols, and the
152 composition of aerosols is key to understanding how aerosols have evolved in the past, and how they will evolve in the
153 future, as some regions are dominated by fossil fuel derived aerosols, which may have peaked in magnitude, while other
154 regions aerosols are driven by agriculture or by natural aerosols (Turnock et al., 2020; Kok et al., 2023). In addition,
155 different aerosols have different impacts on climate, for example, knowing whether aerosols are scattering or absorbing
156 changes the sign of the interaction (Li et al, 2022). Some aerosols also serve as better cloud or ice nuclei than others, while
157 biogeochemical impacts are very sensitive to composition (Mahowald et al., 2011). Knowing the order of magnitude even in
158 regions with aerosols (e.g., contrasting 0.1 to 0.001) is important for aerosol cloud interactions that can be non-linear
159 especially at low aerosol levels (Carslaw et al., 2013). While remote sensing data can provide important information about
160 high aerosol load regions, there is only limited information about the composition (e.g., single scattering albedo under very
161 high aerosol optical depth (AOD>0.4) conditions, for example (Dubovik et al., 2000)). We focus on the spatial distribution
162 of climatological mean, as that is easily obtained from models, and the most important variable for many climate impacts
163 like radiative effects or aerosol-cloud interactions except in cases with large infrequent events (e.g., Clark et al., 2015;
164 Fasulo et al., 2022). The climatological mean is obviously less important for extreme air quality events, or for understanding
165 temporal trends or pollution events, and thus other datasets should be developed for these attributes (e.g., Bowdalo et al.,



166 2024). There have been trends in emissions especially of anthropogenic aerosols over the last 40 years (Quass et al., 2022;
167 Bauer et al., 2022), which we do not access in this study.

168 For this study we focus on the following: a) compiling climatologically averaged means of available PM_{2.5} and
169 PM₁₀ aerosol data, including aerosol composition into a new publicly available database for the modelling community
170 (AEROMAP) across as much of the globe as possible; b) presenting a methodology to compare these observations to an
171 Earth system model; c) identifying the measurement and modelling gaps from this comparison. In this paper, we focus on
172 the climatological average spatial distribution of aerosol particles and key chemical composition information.

173 **2 Description of Methods**

174 **2.1 Observational data**

175 PM observations are made by multiple networks, or during specific field campaigns, and for different size cut-offs, with and
176 without a description of chemical composition. Data was collected by advertising at international meetings (Wiedinmyer et
177 al., 2018), searching the literature, contacting principal investigators and accessing publicly available datasets. As expected,
178 most of the observations are over North America or Europe, with much of the rest of the land areas and most of the ocean
179 much more poorly observed (Fig. 1; Supplemental dataset 1). For this study, we include both PM_{2.5} and PM₁₀ daily (or
180 multiple day averages) data sets that were made available by the investigators or are available from public web sites (Fig. 1;
181 supplemental dataset 1). Some measurement sites measure PM_{2.5} and coarse (PM_{2.5} to PM₁₀) aerosols. For those sites, we
182 convert the latter to PM₁₀ for comparison. Some measurement sites have only a few observations of composition or mass,
183 while others have multiple years: we included less complete datasets at sites in regions with limited data. In some poorly
184 measured regions, we include total suspended particles (TSP) datasets. The time period for different datasets is included in
185 the supplemental dataset 1.

186 Detailed studies have shown that PM₁₀ and PM_{2.5} samplers can differ in the sharpness of their size cut-off (Hand et al.,
187 2019). As an example, comparisons between data from the U.S. Environmental Protection Agency (EPA) Federal Reference
188 Method sites and data from the Interagency Monitoring of Protected Visual Environments (IMPROVE) network show that
189 the coarse matter from collocated sites in both networks were offset by 28% (Hand et al., 2019). There was a bias when data
190 were compared (slope of 0.9), but the correlation coefficient was high (0.9) suggesting overall a good agreement. We focus
191 here on surface station measurements of PM₁₀ and PM_{2.5}, since our model and most models only consider mass up to PM₁₀.
192 For that reason, our model deposition is not directly comparable to observational bulk/total atmospheric deposition since
193 larger particles may dominate the deposition close to the source areas (Kok et al., 2017; Mahowald et al., 2014b; Neff et al.,
194 2013). Measuring absolute dry and wet deposition rates is also technically more challenging (especially dry deposition, since



195 the particles can be re-entrained into the atmosphere), but worthwhile (Heimburger et al., 2012; Prospero et al., 1996). In
196 regions with little data (e.g., outside of North America and Europe) we include measurements of total suspended particulates
197 (TSP) with the PM₁₀, because of the lack of size-resolved data. Data from the Japanese air quality network use a different
198 inlet for the PM10 cutoff as well, which will include a slightly larger size fraction (<https://tenbou.nies.go.jp/download/>).

199 In addition to particulate matter in the PM₁₀ and PM_{2.5} size fractions, we also compile the following observations to compare
200 to the model: black carbon (BC), elemental carbon (EC), organic carbon (OC) (or particulate organic material, OM, that is
201 here considered to be 1.8 x OC in mass), sulfate, nitrate, aluminum, sodium and chloride. To include both BC (based on
202 light absorption measurements) and EC (based on thermal oxidation induced combustion measurements) data are also a
203 source of uncertainty, both are proxies of the soot combustion particles since they are based on different measurements
204 techniques, and there is no accepted equivalence between them (Mbengue et al., 2021). Details on how the model is
205 compared to data for different elements is in section 3.2.

206 For this paper, we focus on the climatological annual means for 1986-2023 which are calculated for all values at each station
207 that are above the detection limit and reported here. At some stations or times, concentrations can be below the detection
208 limit, and excluding these data or time periods could bias our average values. We focus on the stations that have more than
209 50% of the data above the detection limit, and exclude other sites. For those included stations, if the values were reported as
210 below the detection limit, we include in the average one-third of the minimum detection limit. The reported detection limits
211 should bound the upper limit of aerosol mass and allow us to include sites, whose observations were otherwise too low to
212 include, while reducing the potential biasing of our compilation towards higher values (Supplemental dataset 1).

213 2.2 Model description

214 Simulations of aerosol particles were conducted using the aerosol parameterizations within the Community Atmosphere
215 Model, version 6 (CAM6), the atmospheric component of the Community Earth System Model (CESM) developed at the
216 National Center for Atmospheric Research (NCAR) (Hurrell et al., 2013; Scanza et al., 2015; Liu et al., 2012). The aerosol
217 module in this version is closely related to the module used in the Energy Exascale Earth System Model (Golaz et al., 2019;
218 Caldwell et al., 2019). Simulations were conducted at approximately 1°x1° horizontal resolution with 56 vertical layers for
219 four years, with the last three years (2013-2015) used for the analysis (Computational and Information Systems Laboratory,
220 2019). The model simulates three-dimensional transport and wet and dry deposition for gases and particles based on
221 MERRA2 winds (Gelaro et al., 2017).

222 The model included prognostic dust, sea salts, BC, OM, and sulfate particles in the default version, using a modal scheme
223 based on monthly mean emissions for the year 2010 (Liu et al., 2012, 2016; Li et al., 2021). For this study, the coarse size
224 mode (mode 3) was returned to the CAM5 size parameters (geometric standard deviation of 1.8) to better simulate coarse



225 mode particles, and improve the dry deposition scheme and optics used in the model for simulating coarse mode particles
226 like dust as described in Li et al. (2022b).

227 Desert dust is entrained into the atmosphere in dry, sparsely vegetated regions subject to strong winds. We use the Dust
228 Entrainment and Deposition scheme (Zender et al., 2003) with the emitted size distribution given by the updated Brittle
229 Fragmentation Theory (Kok et al., 2014b, a) with improved incorporation of aspherical particles for optics and deposition (Li
230 et al., 2022b; Huang et al., 2021; Kok et al., 2017). Fossil fuel and natural emissions of sulfate, OM, and BC follow the
231 Climate Model Intercomparison Project 6 historical data for 2010 (Gidden et al., 2019).

232 **2.2.1 Modelling of additional aerosol sources and types**

233 The model was modified to allow the addition of several new aerosol particles based on codes with expanded dust speciation
234 (Li et al., 2022b) but here the extra dust tracers are used for the additional species as described below. The additional
235 sources of particles use the same optical properties as bulk dust for this sensitivity study. The following particles were
236 added, and the amount of emissions in each the PM_{2.5} and PM₁₀ sizes and contribution to surface concentration and aerosol
237 optical depth are shown in Table 1. In addition, some of the base case aerosol emissions were modified to match
238 observations, as discussed below.

239 Agricultural sources of dust are added to this version of the model using the same emission scheme as for natural sources
240 (Kok et al., 2014b, a; Li et al., 2022b), but applied to the crop area, and each region is tuned to have the percentage amount
241 of anthropogenic dust to match satellite based observations (Ginoux et al., 2012), except Australia, where other estimates
242 (Bullard et al., 2008; Mahowald et al., 2009; Webb and Pierre, 2018) suggest a lower amount (see Table S1 for comparisons,
243 based on Brodsky et al., 2023). Agricultural dust is separately considered by the model, so its importance can be evaluated.

244 Coarse BC and OC as well as fine and coarse ash from industrial sources were added. Emissions estimated from the GAIN
245 model are added to the model using the ECLIPSEV6_CLE base case (Klimont et al., 2017; Philip et al., 2017). Coarse BC
246 and OM from biomass burning were assumed to be 20% of the fine mode mass (Mahowald et al., 2005).

247 Primary biogenic particles are released from ecosystems either as integral particles, such as bacteria, pollen or spores, or as
248 accidentally entrained leaf pieces (Jaenicke, 2005; Mahowald et al., 2008; Despres et al., 2012; Burrows et al., 2009; Heald
249 and Spracklen, 2009). These sources are poorly observed or understood, and thus looking at coarse mode organic material in
250 this study could provide additional constraints on the budget. Assumptions about size are likely to be very important for the
251 resulting distribution and impacts, e.g., studies show that P budgets are quite different if 5 different size bins or 1 size bin are
252 included in models (Brahney et al., 2015). Four different types of primary biogenic particles were included: bacteria, spores
253 and other miscellaneous emissions (leaf bits, pollen, etc.) from land ecosystems, as well as a marine organic aerosol.



254 Included bacteria sources were read in from a monthly climatology (Burrows et al., 2009). Spore sources were calculated
255 offline and read into the model based on observed leaf area index, temperature, and a source parameterization (Janssen et al.,
256 2020; Heald and Spracklen, 2009). Other terrestrial emissions were estimated based on leaf area index following Mahowald
257 et al. (2008). Marine organic aerosol emissions were included based on the physically based scheme OCEANFILMS
258 (Burrows et al., 2014). Marine organics are externally mixed with sea spray, following Zhao et al. (2021). OCEANFILMS
259 only estimates the fine mode organic mass, and here we assume that the coarse mode marine organic mass equals 1% of the
260 seaspray mass (Gantt et al., 2011). The assumptions about the mass and fraction in each size bin are shown in Table 1.

261 Ammonium nitrate aerosol particles are not included in the standard CAM6 nor in E3SM, but are thought to be important for
262 aerosol optical depth and surface concentrations (Paulot et al., 2016; Adams et al., 1999; Thornhill et al., 2020; Bauer et al.,
263 2007, 2016). Nitrate can also react with dust particles, for example, but that is ignored in this study (Wolf, 2006; Dentener et
264 al., 1996). Ammonium nitrate particles require tropospheric chemistry interactions because the nitrogenous based particles
265 are both a source and a sink for gaseous nitrogen species, which are key elements of tropospheric photochemistry and the
266 particles are in chemical equilibrium with the gas phase (e.g., Nenes et al., 2021; Baker et al., 2021; Bauer et al., 2007;
267 2016), so simulations using the CAM-CHEM model with tropospheric photochemistry are used covering the same time
268 period (Vira et al., 2022). Simulations with chemistry were conducted at $2^\circ \times 2^\circ$ resolution and are linearly interpolated to
269 $1^\circ \times 1^\circ$ resolution used for the other modelled particles. Sulfate in the CAM6 is assumed to be in the form of ammonium
270 sulfate and the nitrate is assumed to be in the form of ammonium nitrate for these studies, so as a rough approximation only
271 the ammonium nitrate needs to be added to consider nitrogenous aerosol optical depth. While aerosol amounts are
272 simulated, ammonium nitrate aerosol optical depth is not calculated within the model but offline. The model does calculate
273 sulfate aerosol optical depth, which has a roughly similar increase in size with humidity, and similar optical properties as
274 long as the nitrates and sulfates are in similar size fractions (Paulot et al., 2016; Bellouin et al., 2020). Therefore the aerosol
275 optical depth from ammonium nitrate (per unit mass) is assumed to be proportional to the sulfate aerosol optical depth per
276 unit mass in each grid box at each time interval. Detailed comparison of the nitrate and ammonia particles, and other species
277 was conducted in Vira et al. (2022). Overall, the model can simulate some of the spatial distribution, but overestimates the
278 nitrate aerosol amounts. This is also seen in Vira et al. (2022), and as shown in Table 1, the calculated nitrate aerosol
279 amounts are multiplied by 0.5 to best match the available observations.

280 2.3 Model-observation comparison methodology

281 Comparisons of the observations to model concentrations were done using BC, OC, SO_4^{2-} , Al, NO_3^- , NH_4^+ , Na, and Cl
282 composition measurements. Some of these elements/compounds map directly onto model constituents (BC, OC, SO_4^{2-} , NO_3^- ,
283 , and NH_4^+), while others serve as proxies for modelled constituents (Al for dust and industrial ash, Na and Cl for sea salts, S
284 for sulfate, etc.). We use non-sea-salt sulfate in ocean regions for estimating sulfate. Some observing networks like



285 IMPROVE use a composite of elements to deduce dust amounts (e.g., Hand et al., 2017). We do not choose to do this for
286 two reasons: 1) at some sites not all the elements are available, and 2) because these elements derive not only from desert
287 dust, but also from industrial sources. Instead, here we explicitly include industrial ash sources and the resulting Al. Note
288 that model values come from the midpoint of the bottom level of the model (~30 m) while the observations are usually taken
289 at 2 or 10 m high. There are several sources of measurement differences between different networks as well as between
290 model and observations. Modelled values of PM content, which assume dry particles, are used, while gravimetric
291 measurements in some networks are equilibrated at 50% relative humidity, thus 5-25% of the mass of measured PM can be
292 water (Prank et al., 2016; Burgos et al., 2020). In addition, comparisons of coarse composition mode composition at co-
293 located sites in the US show that the inlet type can cause ~30% difference in measured mass (Hand et al., 2017).

294 For the most part, we use model output for which there is a on- to-one relationship with what is being measured (BC, sulfate,
295 etc). However, for dust this is not straightforward, as dust is composed of multiple elements. Here we use Al as a proxy for
296 dust, as it is relatively constant (~7%) in dust (as opposed to Ca, which varies highly, or Fe which varies moderately) (Zhang
297 et al., 2015). Al sources are primarily from dust, agricultural dust, road dust and industrial ash emissions; we ignore minor
298 emissions from volcanoes, marine sea spray and primary biogenics for this study (Mahowald et al., 2018). Assumptions
299 about the model composition and how they are compared to observations are shown in Table S2. For example, OM is
300 assumed to be 1.8 times OC.

301 Harmonizing models with different types of measurements is critical (Huang et al., 2021). Models operate with the
302 geometric or aerodynamic particle diameter, whereas in practise the measurements are done with a variety of particle
303 equivalent diameter, e.g., optical, volume equivalent, projected-area equivalent, aerodynamic diameter or electrical mobility
304 diameter, depending on the instrument used (Hinds, 1999; Reid et al., 2003; Rodríguez et al., 2012). In the inlets of the
305 samplers used for the mass-measurements and collection of PM_{2.5} and PM₁₀ particles for subsequent chemical analysis, such
306 size cut-off at 2.5 µm and 10 µm is defined in terms of aerodynamic diameter (i.e., Stokes diameter (involving size and
307 shape) weighed by the square root of the particle density; Hinds, 1999). The sharpness of the cut-off of such inlets
308 influences the PM_{2.5} and PM₁₀ mass concentration (Hand et al., 2019; Wilson et al., 2002). The PM₁₀ size cut-off
309 aerodynamic diameter is equivalent to PM_{6.3} geometric diameter for spherical dust particles (Hinds, 1999; Rodríguez et al.,
310 2012) and to PM_{6.9} in the case of dust aspherical particles (Huang et al., 2021). Similarly, PM_{2.5} (aerodynamic diameter) is
311 equivalent to PM_{1.6} (geometric diameter) for dust. Using standard relationships between the modal particles used in the
312 CAM6 (Liu et al., 2016) and the fraction of the particles below 6.9 µm (Seinfeld and Pandis, 2006) (here referred to as
313 PM_{6.9}), a new diagnostic was added to the model, which shows that in regions with substantial coarse particles like dust,
314 there can be a difference of about 30%, while in most places the differences are less than 5% (Fig. S1). These assumptions
315 are less true for coarse particles like sea salts, but the differences are small in sea salt dominated regions (Fig. S1). For this



316 study we use PM_{6.9} from the model. Note that the inlet size discrimination for PM_{2.5} measurements are also not a step
317 function and also this might affect the comparisons for PM_{2.5}.

318 For ease of viewing the data in this paper in the densely sampled regions as well as to compare model output to more
319 representative spatial scales, observational records from different sites were combined into a mean within a grid cell that is
320 two times the model resolution, or approximately 2° x 2°. This process averages the observations over a spatial scale
321 appropriate for comparison with the chemistry model (Schutgens et al., 2016). We provide both the climatological annual
322 average data at each site as well as the averaged data (with the modelled data at doi: 10.5281/zenodo.10459654, Mahowald
323 et al., 2024).

324 Notice that we include both urban regions and rural or remote sites into the same dataset. Some of the original meta data did
325 not include the resolution of the location to better than 0.25 degrees, so that the coordinates of the locations here provided
326 with the gridded data should not be used for finer resolution studies. Because of the importance and size of megacities,
327 which cross multiple grid boxes, we include urban and rural air quality data in the same dataset, and previous studies show
328 the expected differences between urban and rural concentrations and trends (e.g., Hand et al., 2019).

329 There are multiple sources of uncertainties in the observations used in the model-data comparisons of PM concentrations at
330 the global model grid scale: errors in the measurements, differences in measurement methods, variability in aerosol
331 concentrations during events versus background conditions, spatial variability within a model grid box, and interannual
332 variability. To assess the size of these uncertainties, we look at the normalized standard deviation (defined as the standard
333 deviation over the mean) due to these factors in the observations for within year, with in a 2°x2° degree grid and for
334 interannual variability. To evaluate within year and between year variability, we focus on stations that have more than 10
335 years of data. To evaluate spatial variability within grid boxes, we use grid boxes that have more than 10 stations within
336 them. Notice that these grid boxes are likely to lie close to cities and fossil fuel source regions, because the measurement
337 network is more dense there, perhaps exaggerating the importance of spatial variability. In addition, different measurement
338 methods (dry vs. moist aerosol mass different inlet geometries) complicate the comparisonl of data. We assume here a
339 measurement method uncertainty of 30% that is on the high side of previous studies (Prank et al., 2016; Burgos et al., 2020;
340 Hand et al., 2017). Many of the measurements also include an assessment of their uncertainty or of the minimum detected
341 limit: we use that to assess the average uncertainty of individual measurements (measurement errors).



342 3 Results

343 3.1 AEROMAP observational data set

344 First, we assessed the amount of data and the number of stations within each $\sim 2^\circ \times 2^\circ$ gridded area (Fig. 1). The
345 observational dataset provides coverage predominately over North America and Europe for $\text{PM}_{2.5}$ and PM_{10} , as noted by
346 previous studies (e.g., Szopa et al., 2021), but in addition we provide here a synthesis of more air quality data in other
347 regions, especially Asia (Fig. 1). This data set comprises most of the individual observations (at daily or higher time
348 periods) of total $\text{PM}_{2.5}$ (Fig. 1a, 1e: blue bars) and most of the observing stations (Fig. 1e and blue line). Approximately
349 15,000 stations and over 20 million observations are included in this compilation as annual averages.

350 Notice that there are two to three orders of magnitude more daily observations for the total mass (PM) of particles compared
351 to information about the composition of particles (Fig. 1e), which is shown also by contrasting the spatial distribution of
352 measurements between $\text{PM}_{2.5}$ and measured amounts of OM (Fig. 1a versus 1b), as well as a large difference between the
353 number of stations measuring the total mass versus the speciated aerosol particles like OM (Fig. 1c versus 1d). While this
354 dataset presents a huge increase in the amount of data available to the aerosol modelling community, still the dominant
355 proportion of the total $\text{PM}_{2.5}$ or PM_{10} data are clustered over a few regions, and there is little composition information over
356 most of the globe (Fig. 1).

357 3.2 Uncertainties in spatial aerosol distributions

358 Our goal in this study was to provide observational constraints on particles that vary spatially over 4-5 orders of
359 magnitude globally (Mahowald et al., 2011). To do that we collect all available datasets, prioritizing long term stations with
360 composition data, but in regions with few measurements, we include only PM data, or data collected during field campaigns,
361 which may last only a month or two. Previous studies have shown that even a 1 day average aerosol measurements, carried
362 out on cruises, can constrain aerosol concentrations within a order of magnitude (1-sigma) for phosphorus in dust, which varies
363 spatially by 4 orders of magnitude (Mahowald et al., 2008). Other studies have highlighted that even for particles that have
364 highly variable sources, such as dust, that only a few months of observations are enough to characterize the mean and standard
365 deviation in most places across the globe (Smith et al., 2017). However, that study highlighted that places where dust events
366 do not occur every year, like near South America, several years are required to characterize the mean (Smith et al., 2017).
367 Thus, the dataset described here cannot do a good job of constraining aerosol concentrations that are due to episodic emission
368 events like wildfires or dust in regions without long term datasets.

369 Uncertainties in the observations used in the comparisons of aerosols at the global model grid scale come from
370 multiple sources: errors in the measurements, differences in measurement methods, variability in aerosol concentrations during
371 events versus background conditions, spatial variability within a model grid box, and interannual variability, as discussed in
372 Section 2.3. To assess the size of the variability contribution to the uncertainties, we look at the normalized standard deviation



373 (defined as the standard deviation over the mean) due to these factors in the observations for within year, with grid and
374 interannual variability. In addition, different measurement methods (dry vs. moist aerosol mass different inlet geometries)
375 complicate the comparison of data. We assume here a measurement method uncertainty of 30% that is on the high side of
376 previous studies (Prank et al., 2016; Burgos et al., 2020; Hand et al., 2017). Many of the measurements also include an
377 assessment of their uncertainty or of the minimum detected limit: we use that to assess the average uncertainty of individual
378 measurements (measurement errors).

379 The largest uncertainties are associated with within-year variability (0.45) (Figure 1g). Uncertainty due to combining
380 different measurement methods (0.3) and from spatial variability within a model grid cell (0.23) are also important (Figure
381 1g). Both interannual variability (0.12) and measurement errors (0.1) are smaller but important contributions to uncertainty.
382 The importance of within year variability is consistent with studies showing that in most places, there are a few pollution
383 events carrying much of the mass, and with otherwise much lower background concentrations (Luo et al., 2003; Fiore et al.,
384 2022). Obviously, interannual variability is important for secular trends (Gupta et al., 2022; Watson-Parris et al., 2020), but
385 tends to be much smaller than the 2-4 orders of magnitude of the spatial variability across the globe, and thus can be neglected
386 for understanding global spatial distributions (Figure 1g).

387 These sources of uncertainties occur simultaneously and if we sum them assuming orthogonality, we obtain an
388 normalized uncertainty of 0.6, which was interpreted as meaning that model/data comparisons within a factor of three should
389 be considered adequate. To ease the visual evaluation of the comparison we show in the following scatter plots both the 1:1
390 line and the range within a factor of 3. We discuss an example of uncertainties in more detail in Section 3.3. Notice that if we
391 use the same metric (normalized standard deviation) to evaluate the variability across the climatological concentrations
392 measured in the observations at different locations (Figure 2a) or across the grid averages in the model we obtain 1.0 and 2.2,
393 respectively, much larger than the uncertainties (0.6): there is much more variability across different grid boxes (4-5 orders of
394 magnitude) than in time (up to 50%). As expected, the model contains more spatial variability than the observations, as the
395 model reports concentrations in very high (North Africa) and very low (Antarctica) aerosol regions where we have no data.

396 **3.3 PM_{2.5} model-data comparison**

397 Modelled concentrations of PM_{2.5} are more often compared against observations than for PM₁₀ or other size fractions, and
398 comprise an important portion of the particulate matter associated with human activities. Therefore, we describe first the
399 observational synthesis and comparison to model results for PM_{2.5}. Because the high number of observations in some parts of
400 the world would make the figures unreadable, the observations are gridded onto an approximately 2°x2° grid for
401 comparisons with the model (Fig. 2a). As expected, in the model the highest concentrations are over the desert dust regions,
402 such as North Africa, and over heavily industrialized regions in Asia. For the heavily industrialized regions in Asia, these
403 high values are consistent with the observations, but the regions in North Africa with the highest modelled values do not
404 have similar observational validation for high concentration values due to a lack of data (Fig. 2a).



405 Overall, the model is able to simulate much of the spatial variability in PM_{2.5} over two orders of magnitude (Fig. 2a and 2c),
406 however there is an overestimate in the PM_{2.5} over India and China (Fig. 2b), which for some observations is outside the x3
407 uncertainty estimates (Figure 2c and 2d). As an example of the source of the uncertainties discussed in Section 3.2, we
408 discuss these in more detail. It seems likely that at least some of these errors are due to an overestimate in the emission
409 databases, since satellite based remote sensing has shown an overestimate in SO₂ over China (Luo et al., 2020). In addition,
410 these discrepancies could be due to an error in the aerosol transport modelling or the time period: the observations are more
411 recent while the assumptions for the emissions are for the year 2010. In addition, notice that once averaged over the 2x2
412 grids more observations are within a factor of 3, our uncertainty (contrast 2c and 2d). However, there could also be
413 methodological and analytical differences due to which group or network did the observations or the exact locations of the
414 different monitors. Much of the data in those regions are not usually included in compilations of data, so the fact that
415 previous model studies have not been able to assess emission datasets in these regions could explain this discrepancy.
416 Comparison between different observations in some cities (Fig. 3) shows that in these grid boxes there can be very large
417 differences (~factor of 3) between the annually averaged values reported at nearby stations within 1° distance radially.
418 Notice that the AirNow measurements (<https://www.airnow.gov/international/us-embassies-and-consulates/> on the US
419 embassies) tend to be higher than those reported from government air quality networks. The sites compared are in large cities
420 and thus are likely to have strong local sources and intense gradients in pollutants. For now, we keep in mind this large
421 difference, but continue to use the observations. As indicated below, in these regions we do not have measurements of
422 composition so we do not know which constituents are poorly simulated in our emissions or transport modelling. More
423 statistics describing the model data comparisons are shown in Table S4.

424 The scatterplots show the comparisons of the model to the observations using the gridded data (Fig. 2c) and all original data
425 (Fig. 2d), and the correlation coefficients are similar (0.73 vs. 0.78 in Fig 2c and Fig 2d, respectively).

426 Next, we consider the composition of the PM_{2.5} aerosol in the model versus the observations, starting with the aerosol
427 components in the default version of the model. Sulfate particles tend to be overestimated in the model in North America,
428 but not over Europe and other regions (Fig. 4a and b). Previous studies have compared SO₄²⁻ aerosol observations to some
429 model simulations and have not noted this bias (e.g., Barrie et al., 2001; Aas et al., 2019) but this bias was seen in this model
430 (Liu et al., 2012; Yang et al., 2018). BC comparisons suggest the model results are roughly able ($r=0.25$, within the x3
431 uncertainty) to capture the spatial dynamics of this aerosol across more than 2 orders of magnitude (Fig. 4c and d). This is
432 similar to previous model intercomparisons (Koch et al., 2009; Bond et al., 2004, 2013; Liu et al., 2012, 2016). Simulations
433 of OM in the default model suggest that the model is within the uncertainty of most of the data. Correctly modelling organic
434 material is very difficult both due to the sparsity of data for comparison, as well as the importance of both primary and
435 secondary OM in PM (Heald et al., 2010; Kanakidou et al., 2005; Olson et al., 1997; Tsigaridis et al., 2014), and previous
436 studies with this model have noted an overestimate in comparison with surface observations (Liu et al., 2012). In our study



we include primary biogenic particles, which are usually not included in model studies (Mahowald et al., 2011, 2008; Jaenicke, 2005; Heald and Spracklen, 2009; Burrows et al., 2009; Myriokefalitakis et al., 2016), but these are a very small part of the PM_{2.5} and occur mostly in the coarse fraction (Table 1) and thus are not causing any bias, which must be due to biomass burning and/or industrial emissions.

As a proxy for sea salts, we use the elemental data of the major component, Na, and although most of the data is within the uncertainties, the model tends to be too high at low Na and too low at high Na in North America, where much of the data are available (Fig. 4g and h), which has been seen previously with this model (Liu et al., 2012). Notice that we do not include industrial emissions of Na as they have not been spatially estimated. As a proxy for dust, we use Al amounts (Fig. 4i and j), which globally and over dust regions are dominated by dust, although there are few observational datasets in high dust regions. The comparisons suggest the model is able to simulate dust across 4 orders of magnitude, similar to previous studies (Liu et al., 2012; Albani et al., 2014a; Li et al., 2022b; Huneeus et al., 2011) although there is a tendency for a high bias in the models over low dust regions and a low bias in high dust regions, similar to sea salts (Fig. 4i and 4.j).

Next, we consider the nitrogen aerosol ammonium nitrate that requires complicated gas-aerosol phase equilibrium to correctly simulate (e.g., Bauer et al., 2007; Thornhill et al., 2021; Adams et al., 2001; Regayre et al., 2018; Seinfeld and Pandis, 2006). To summarize these complicated interactions, because SO₄²⁻ is a stronger acid than NO₃⁻ in the atmosphere, the basic NH₄⁺ is preferentially found with SO₄²⁻. Thus NO₃⁻ particles will only form if there is sufficient NH₄⁺ available, therefore the ratio of NO₃⁻ to total NH₄⁺ can vary. As described in the methods, to include these particles we used simulations from a different version of the same model which include chemistry (Vira et al., 2022), and a more process-based source of ammonia (Vira et al., 2020) since the default CESM2 version used here for most particles does not include chemistry. Note that even in the chemistry version of the model for CESM2 the complicated gas-aerosol phase equilibrium is not included, which causes errors in the simulation of the amounts of nitrogen aerosol (e.g., Bauer et al., 2007; Thornhill et al., 2021; Adams et al., 2001; Regayre et al., 2018; Nenes et al., 2021). Thus while the NH₃ agricultural emission scheme used in this model is state-of-the-art, the lack of an adequate gas-aerosol phase separation may lead to biases as discussed in Vira et al. (2022). In addition, recent studies have suggested that emissions of NH₄ from vehicles should be 1.8x higher than previously estimated (Toro et al., 2024), highlighting the difficulty of adequate emission datasets for nitrogenous aerosol precursors. NO₃⁻ particles compared against available observations show that over 2 orders of magnitude, the model results are able to simulate the spatial variability, with most of the data within the uncertainties (Fig. 4k and l). Note that here, we have multiplied the simulations by a factor 0.5 in order to achieve a better mean comparison, as indicated by Vira et al. (2022). In addition, NH₄⁺ results show the importance of NH₄⁺ over agricultural regions especially (e.g., Vira et al., 2022), and that the NH₄⁺ in the simulation used here compares well to available observations by being within the uncertainties at most observational sites (Fig. 4m and n; Vira et al., 2022).



468 **3.4 PM₁₀ model-data comparison**

469 PM₁₀ was the first size selective standard for particulate air quality until more studies showed that smaller particles (PM_{2.5} or
470 PM₁) were more relevant for health impacts and PM_{2.5} standards were added (e.g., <https://www.epa.gov/pm-pollution/timeline-particulate-matter-pm-national-ambient-air-quality-standards-naaqs>, accessed October 4, 2023).

471 However, there are still many PM₁₀ measurements routinely made (Fig 1d; Fig. 5a). As discussed in the methods, what is
472 described as measurements of PM₁₀ (aerodynamic diameter) is probably closer to PM_{6.9} (geometric diameter) as simulated in
473 models (Huang et al., 2021), so here we use the PM_{6.9} fraction as calculated in the model to compare to PM₁₀ observations
474 (Fig. S1 shows the fraction of PM₁₀ that is PM_{6.9}. This distinction is only important in regions with substantial coarse mode
475 emissions like desert dust source regions. For marine coarse aerosols like sea salt, the distinction between geometric and
476 aerodynamic diameter may be smaller.). The model is able to simulate PM₁₀ concentrations across 2 orders of magnitude
477 with some skill, as most of the data is within the uncertainties (Fig. 5a, c and d), although the region of East Asia, especially
478 China and India are overestimated in the model similar to the PM_{2.5} (Fig. 3a, and b). Gridding the data before comparing to
479 the model results in a similar correlation across space as including all data (Fig 5b vs. c). More statistical comparisons are
480 shown in Table S5.

481

482 There are fewer comparisons with PM₁₀ composition data available in the literature: usually only sea salts and dust are
483 compared to observations that include the coarse mode (Gong et al., 2003; Ginoux et al., 2001; Albani et al., 2014b;
484 Mahowald et al., 2006). Comparisons for SO₄²⁻ suggest that the model tends to over predict PM₁₀ values in some locations,
485 as many observations are too high and outside the uncertainty bounds (Fig. 6a and b.). For BC, the PM₁₀ simulation captures
486 the range of values, with most of the data within the uncertainty bounds (Fig. 6c and d in contrast to a and b.). Unlike many
487 studies we include BC in the PM₁₀ mode, since observations show that there are some contribution of BC to PM₁₀ (compare
488 Fig. 6c versus 4c). The model simulations for OM include primary biogenic particles and the limited available observations
489 do not support larger sources of OM in the PM₁₀, than included here (as suggested in e.g., Jaenicke, 2005): indeed the model
490 is overestimating the OM in PM₁₀ at many stations especially in North America. Similarly, the limited Na (indicating sea
491 salt) data suggest the model in some places may overestimate Na even over continents outside the error bound (Fig. 6g and
492 h), as discussed in the PM_{2.5} section, as was seen previously (Liu et al., 2012). Comparisons with Al (proxy for dust) show
493 that the variability is well simulated, but the model overpredicts the concentrations. Dust models are compared against
494 aerosol optical depth at stations and using global averages of deposition and surface concentrations and it is currently not
495 possible to simulate all of these at the same time, consistent with previous studies with this model (Li et al., 2022b; Kok et
496 al., 2014b; Albani et al., 2014a; Matsui and Mahowald, 2017; Zhao et al., 2022), and indeed across most dust models
497 (Huneeus et al., 2011).

498

499



500 For the particulate NO_3^- , similar to the $\text{PM}_{2.5}$ size, the particles were multiplied by 0.5 to better match the observations
501 following Vira et al. (2022) (Fig 6k and l). The model simulations suggest too high values in high NO_3^- areas, and too low in
502 low NO_3^- regions (Fig. 6k and l). NH_4^+ shows a slightly better comparison to the limited available data (Fig. 6m and n) as
503 seen in Vira et al. (2022). As discussed earlier, the model does not include other forms of nitrate aerosols which may be
504 important, such as the reaction of nitrate with dust aerosols (Wolff, 1984; Dentener et al., 1996; Xu and Penner, 2012;
505

506 **3.5 Data and model coverage**

507 The compilation shown here is the most comprehensive currently available for describing the spatial variability of the total
508 mass and composition of in situ particulate concentration data, and yet it highlights the lack of sufficient data to constrain the
509 current distribution of particles and their composition (Fig. 7a and b). Only 3% of the grid boxes ($2^\circ \times 2^\circ$) have $\text{PM}_{2.5}$ data
510 (about 10% of land grid boxes), and only 0.3% has sufficient data to constrain most of the composition (defined as having
511 90% of the variables considered here: total mass, SO_4^{2-} , BC, OM, Na or Cl, Al or dust, NO_3^- and NH_4^+). There are even less
512 data available to characterize PM_{10} , which is less important for air quality and aerosol-cloud interactions but more important
513 for aerosol-biogeochemistry interactions and long wave interactions (Mahowald et al., 2011; Li et al., 2022a; Lim et al.,
514 2012; Kanakidou et al., 2018). Because of the high spatial and temporal variability and the lack of satellite or other remote
515 sensing data to characterize the type of aerosol, this lack of data is a severe handicap in constraining aerosol radiative forcing
516 uncertainties and other impacts of particles in the climate system.

517 In this simulation, we included several new aerosol sources and types that are not in the default model to investigate their
518 importance. For the CESM this simulation includes agricultural dust, nitrogen particles and several other sources (see Table
519 1). As shown in Fig. 8, the default particles are the dominant particles over most of the planet, but in many regions for both
520 $\text{PM}_{2.5}$ and PM_{10} , the default aerosol scheme includes less than 30% of the aerosol particles (Fig. 8a and c), with substantial
521 contributions from the new added particles (Fig. 8b and d), especially nitrogen particles and agricultural dust. Many Earth
522 system or climate models such as the CESM2 do not include nitrogen particles (NO_3^- and NH_4^+), because of the substantial
523 complexity and computation load of chemistry and gas-aerosol equilibrium (Bauer et al., 2007; Thornhill et al., 2021; Adams
524 et al., 2001; Regayre et al., 2018)). Previous studies have highlighted the importance of nitrogen particles for climate, air
525 quality and ecosystem impacts (e.g., Adams et al., 2001; Bauer et al., 2007, 2016; Kanakidou et al., 2016; Baker et al.,
526 2021). Changes in nitrogen aerosol emissions are likely to follow different future trajectories than SO_4^{2-} , BC or OC, whose
527 anthropogenic sources are mostly fossil fuel derived and should decrease in the future as renewable energy resources expand
528 (Gidden et al., 2019). Ammonia has substantial sources from agriculture, which will likely to stay constant or expand
529 (Gidden et al., 2019; Klimont et al., 2017; Bauer et al., 2016). This suggests there could be a substantial bias in both
530 historical and future aerosol forcings due to the lack of inclusion of these important sources (e.g., Bauer et al., 2007;
531 Thornhill et al., 2021; Adams et al., 2001; Regayre et al., 2018).



532 **4. Conclusions**

533 In this study, we present a new aerosol compilation (AERO-MAP) designed to evaluate the spatial variability of particulate
534 matter in Earth system and air quality models. This climatologically averaged dataset includes both total mass and
535 composition, where available, including 15,000 station datasets and over 10 million daily to weekly averaged measurements.
536 Spatial variability represents the largest source of variability in aerosols (Figure 1f and Section 3.2), and thus the most
537 important to simulate accurately in models, especially as some climate effects are strongly non-linear, and knowing small
538 concentrations ($1 \mu\text{g}/\text{m}^3$) versus very small concentrations ($0.1 \mu\text{g}/\text{m}^3$) is important (Carslaw et al., 2013). Here we expand
539 beyond the usual limited coverage of only North America and Europe to present a more global data view for both PM_{2.5} and
540 PM₁₀ (Fig. 1). Unfortunately, there are still very limited data characterizing both the surface concentration, size and
541 composition of aerosol particles (Fig. 7). While satellite remote sensing can indicate the total atmospheric loading during
542 cloud free conditions, it cannot yet provide substantial information about the size or composition of particles (Kahn et al.,
543 2005; Tanré et al., 1997; Remer et al., 2005). Surface based remote sensing may provide more information about size and
544 absorption properties (Holben et al., 1991; Dubovik et al., 2002; Schuster et al., 2016; Gonçalves Ageitos et al., 2023; Obiso
545 et al., 2023), but single scattering albedo, for example, is only available under very high (>0.4 AOD) aerosol loading
546 conditions, and thus is not available most of the time and space (Dubovik et al., 2002). Knowing the size and the
547 composition of aerosols is key to their impacts on air quality and climate (Mahowald et al., 2011). Knowing what
548 particulates are dominant in a region is required, as fossil fuel derived aerosols will be reduced, while agriculturally based
549 aerosols may well increase (Gidden et al., 2019). We also present a method that is generalizable to other models to use this
550 dataset to evaluate both mass and composition for intercomparison projects and improvements in air quality and Earth
551 system models.

552 This study has highlighted the value of surface concentration data, but represents only the climatological mean values
553 showing the spatial variability, while there is also information in the temporal variability of the PM. A recent, independent
554 and complementary effort collects all atmospheric composition data (not just aerosols) from many networks into one easy to
555 use framework called GHOST (Globally harmonised dataset of surface atmospheric composition measurements; Bowdalo et
556 al., 2024). The approach used in GHOST includes presenting the data in netcdf format, at the original resolution, with meta
557 data about measurement type, etc. included, and is an important step forward (Bowdalo et al., 2024). At this point GHOST
558 only includes a subset of the data available in this study: we hope that the GHOST effort can be expanded to include more
559 spatial variability and be maintained into the future.

560 This study also highlights the importance of including all aerosol components into the models, and shows that in the
561 CESM2, in many places there is between 10-60% of the particulate mass missing, largely due to lack of the nitrogenous
562 particles (Paulot et al., 2016; Adams et al., 1999; Thornhill et al., 2020) and the poorly understood agricultural dust particles
563 (e.g., Ginoux et al., 2012). Because these particles are largely driven by agricultural sources and not fossil fuels, their



564 concentrations will be hardly affected by the transition to renewable energy and may increase if agricultural production
565 expands with population. Therefore, these aerosol particles represent important air quality and climate impacts that should
566 be represented more accurately in future studies.

567 **Data availability:** The data compiled here is available as a csv table with citations as a supplemental data. This same file is
568 available as well as gridded datasets with the modelled data in netcdf format at <https://zenodo.org/records/10459654>,
569 **10.5281/zenodo.11391232** Mahowald et al., 2024. Additional underlying datasets available by request to
570 mahowald@cornell.edu.

571 **Code availability:** The model used here is a version of the Community Earth System Model, and the modifications and input
572 files to that code are available at <https://zenodo.org/records/10459654>, Mahowald et al., 2024.

573 **Author contributions:** NMM designed and oversaw the implementation of the approach with the advice of HL, CW, RVM
574 and JL, and wrote the first draft of the manuscript. JV, PH, LLi, ZK, CD, SR, TB and DH assisted in the version of the
575 model and emission datasets used. EA, DM, HM and LLu authors assisted in the compilation and conversion of the data,
576 CH, ZKl contributed emission datasets, XL and XZ contributed model code, MGA, CA, AA, PA, AB, FB, SB, GC, SC, YC,
577 PC, DC, CC, ED, GD, KE, CG-L, CG, DG, YGR, HH, RH, CH, BH, PH, CH, MK, ZKe, KK, FL XL, RL, RL, WM, BM,
578 RM, NM, YM-G, AP, JP, SR, PS, DV, BW authors contributed data. All authors edited the manuscript.

579 **Competing interests:** The authors declare that the only conflict of interest is that Maria Kanakidou, Xiaohong Liu, Willy
580 Maenhaut, and Sergio Rodriguez are editors at Atmospheric Chemistry and Physics.

581 Acknowledgments

582 NMM and LL would like to acknowledge support from DOE (DE-SC0021302), as well as from Paul Ekhart (EBAS), the
583 many freely available air quality websites acknowledged in the paper: EBAS (<https://ebas.nilu.no/>)--including data affiliated
584 with ACTRIS (Aerosol Clouds and Trace gas Research Infrastructure), EMEP (European Monitoring and Evaluation
585 Programme), GAW-WDCA (Global Atmosphere Watch-World Data Centre for Aerosols), EANET Acid Deposition
586 Monitoring Network in (East Asian)--All Indian Air Quality Management data ([https://app.cpcbccr.com/CCR/#/caaqm-
587 dashboard-all/caaqm-landing/data](https://app.cpcbccr.com/CCR/#/caaqm-dashboard-all/caaqm-landing/data)), Australian National Air Pollution Monitoring Database (<https://osf.io/jxd98/>), South
588 African Air Quality Information System (<https://saaqis.environment.gov.za/>), Mexico City Air quality data



589 (<http://www.aire.cdmx.gob.mx/default.php?opc=%27aKBh%27>), Chile (Sistema de Informacion Nacional de Calidad del
590 Aire--<https://sinca.mma.gob.cl/index.php/>), Japan's NIES (National Institute for Environmental studies-
591 <https://tenbou.nies.go.jp/download/>), Turkey Air Quality Monitoring Network, Israel Air Quality Monitoring website, US
592 EPA CASNET and IMPROVE, US AIRNOW, New Zealand Stats now website, Chilean
593 (<https://www.stats.govt.nz/indicators>), Chinese Air Quality data collected together (<https://osf.io/jxd98/>) and Canadian
594 National Air Quality Surveillance (<https://data.ec.gc.ca/data/air/monitor/national-air-pollution-surveillance-naps-program/Data-Donnees>). FB and FL would like to acknowledge support from the Ministerio del Medio Ambiente de Chile
595 (<https://mma.gob.cl>) and Fondecyt 1231682. SC is grateful for financial support from the Texas Air Research Center and the
596 Texas Commission on Environmental Quality. PA acknowledges funding from Fundação de Amparo à Pesquisa do Estado
597 de São Paulo (FAPESP), grants number 2017-17047-0 and 2023/04358-9. RVM acknowledges funding from NSF Grant
598 2020673. MK and NM acknowledge support by Greece and the European Union (European Regional Development Fund)
599 via the project PANhellenic infrastructure for Atmospheric Composition and climatE chAnge (PANACEA, MIS 5021516).
600 CGL and BM acknowledge support of CNRS, IRD and ACTRIS-France to the International Network to study Atmospheric
601 Deposition and Atmospheric chemistry in AFrica programe (INDAAF). HM acknowledges support by the MEXT/JSPS
602 KAKENHI Grant Numbers JP19H05699, JP19KK0265, JP20H00196, JP20H00638, JP22H03722, JP22F22092,
603 JP23H00515, JP23H00523, and JP23K18519, the MEXT Arctic Challenge for Sustainability phase II (ArCS II;
604 JPMXD1420318865) project, and by the Environment Research and Technology Development Fund 2-2301
605 (JPMEERF20232001) of the Environmental Restoration and Conservation Agency. RLM acknowledges support from the
606 NASA Modeling, Analysis and Prediction Program. We acknowledge contributions from Sagar Rathod, Tami Bond, Giles
607 Bergametti, Javier Miranda Martin del Campo, and Xavier Querol. The support to CESAM by FCT/MCTES
608 (UIDP/50017/2020+UIDB/50017/2020+ LA/P/0094/2020) is also acknowledged.
609
610
611

612 References

613 Aas, W., Mortier, A., Bowersox, V., Cherian, R., Faluvegi, G., Fagerli, H., Hand, J., Klimont, Z., Galy-Lacaux, C.,
614 Lehmann, C. M. B., Myhre, C. L., Myhre, G., Olivié, D., Sato, K., Quaas, J., Rao, P. S. P., Schulz, M., Shindell, D.,



- 615 Skeie, R. B., Stein, A., Takemura, T., Tsyro, S., Vet, R., and Xu, X.: Global and regional trends of atmospheric
616 sulfur, *Sci Rep*, 9, <https://doi.org/10.1038/s41598-018-37304-0>, 2019.
- 617 Adams, P., Seinfeld, J., and Koch, D.: Global concentrations of tropospheric sulfate, nitrate and ammonium aerosol
618 simulated in a general circulation model, *J. Geophysical Research*, 104, 13791–13823, 1999.
- 619 Adams, P., Seinfeld, J., Koch, D., Mickley, L., and Jacob, D.: General circulation model assessment of direct radiative
620 forcing by sulfate-nitrate-ammonium-water inorganic aerosol system, *J Geophys Res*, 106, 1097–1111, 2001.
- 621 Adebiyi, A., Kok, J. F., Murray, B. J., Ryder, C. L., Stuut, J.-B. W., Kahn, R. A., Knippertz, P., Formenti, P., Mahowald, N.
622 M., Pérez García-Pando, C., Klose, M., Ansmann, A., Samset, B. H., Ito, A., Balkanski, Y., Di Biagio, C.,
623 Romanias, M. N., Huang, Y., and Meng, J.: A review of coarse mineral dust in the Earth system, *Aeolian Res*, 60,
624 100849, <https://doi.org/10.1016/j.aeolia.2022.100849>, 2023.
- 625 Alastuey, A., Querol, X., Aas, W., Lucarelli, F., Pérez, N., Moreno, T., Cavalli, F., Areskoug, H., Balan, V., Catrambone,
626 M., Ceburnis, D., Cerro, J. C., Conil, S., Gevorgyan, L., Hueglin, C., Imre, K., Jaffrezo, J. L., Leeson, S. R.,
627 Mihalopoulos, N., Mitosinkova, M., O'Dowd, C. D., Pey, J., Putaud, J. P., Riffault, V., Ripoll, A., Sciare, J.,
628 Sellegri, K., Spindler, G., and Yttri, K. E.: Geochemistry of PM10 over Europe during the EMEP intensive
629 measurement periods in summer 2012 and winter 2013, *Atmos Chem Phys*, 16, 6107–6129,
630 <https://doi.org/10.5194/acp-16-6107-2016>, 2016.
- 631 Albani, S., Mahowald, N. M., Perry, A. T., Scanza, R. A., Zender, C. S., Heavens, N. G., Maggi, V., Kok, J. F., and Otto-
632 Bliesner, B. L.: Improved dust representation in the Community Atmosphere Model, *J Adv Model Earth Syst*, 6,
633 541–570, <https://doi.org/10.1002/2013MS000279>, 2014a.
- 634 Albani, S., Mahowald, N., Perry, A., Scanza, R., Zender, C., and Flanner, M. G.: Improved representation of dust size and
635 optics in the CESM, *Journal of Advances in Modeling of Earth Systems*, 6, doi:10.1002/2013MS000279, 2014b.
- 636 Almeida, S. M., Pio, C. A., Freitas, M. C., Reis, M. A., and Trancoso, M. A.: Source apportionment of fine and coarse
637 particulate matter in a sub-urban area at the Western European Coast, *Atmos Environ*, 39, 3127–3138,
638 <https://doi.org/10.1016/j.atmosenv.2005.01.048>, 2005.
- 639 Amato, F., Alastuey, A., Karanasiou, A., Lucarelli, F., Nava, S., Calzolai, G., Severi, M., Becagli, S., Gianelle, V. L., Colombi,
640 C., Alves, C., Custódio, D., Nunes, T., Cerqueira, M., Pio, C., Eleftheriadis, K., Diapouli, E., Reche, C., Minguillón,
641 M. C., Manousakas, M. I., Maggos, T., Vratolis, S., Harrison, R. M., and Querol, X.: AIRUSE-LIFE+: A harmonized
642 PM speciation and source apportionment in five southern European cities, *Atmos Chem Phys*, 16, 3289–3309,
643 <https://doi.org/10.5194/acp-16-3289-2016>, 2016.
- 644 Andreae, T. W., Andreae, M. O., Ichoku, C., Maenhaut, W., Cafmeyer, J., Karnieli, A., and Orlovsky, L.: Light scattering by
645 dust and anthropogenic aerosol at a remote site in the Negev desert, Israel, *Journal Geophysical Research*, 107,
646 <https://doi.org/10.1029/2001JD900252>, 2002.
- 647 Arimoto, R., Duce, R. A., Ray, B. J., and Tomza, U.: Dry deposition of trace elements to the western North Atlantic, *Global
648 Biogeochem Cycles*, 17, <https://doi.org/10.1029/2001GB001406>, 2003.



- 649 Artaxo, P. and Maenhaut, W.: Aerosol characteristics and sources for the Amazon Basin during the west season, *J Geophys*
650 *Res*, 95, 16971–16985, 1990.
- 651 Artaxo, P., Martins, J. V., Yamasoe, M. A., Procopio, A. S., Pauliquevis, T. M., Andrae, M. O., Guyon, P., Gatti, L. V., and
652 Leal, A. M. C.: Physical and chemical properties of aerosol particles in the wet and dry seasons in Rondonia,
653 Amazonia, *J Geophys Res*, 107, 8081, doi: 10.1029/2001JD0000666, 2002.
- 654 Baker, A.R., Kanakidou, M., Nenes, A., Myriokefalitakis, S., Croot, P. L., Duce, R.A., Yuan Gao, Y., Guieu, C., Ito, A.,
655 Jickells, T.D., Mahowald, M.A., Middag, R., Perron, M.M.G., Sarin, MM., Shelley, R., Turner D.R: Changing
656 atmospheric acidity as a modulator of nutrient deposition and ocean biogeochemistry, *Science Advances*, 2021 (7)
657 eabd8800, 2021
- 658 Barkley, A. E., Prospero, J. M., Mahowald, N., Hamilton, D. S., Popendorf, K. J., Oehlert, A. M., Pourmand, A., Gatineau,
659 A., Panechou-Pulcherie, K., Blackwelder, P., and Gaston, C. J.: African biomass burning is a substantial source of
660 phosphorus deposition to the Amazon, Tropical Atlantic Ocean, and Southern Ocean, *Proceedings of the National
661 Academy of Sciences*, 116, 16216–16221, <https://doi.org/10.1073/pnas.1906091116>, 2019.
- 662 Barraza, F., Lambert, F., Jorquera, H., Villalobos, A. M., and Gallardo, L.: Temporal evolution of main ambient PM2.5
663 sources in Santiago, Chile, from 1998 to 2012, *Atmos Chem Phys*, 17, 10093–10107, <https://doi.org/10.5194/acp-17-10093-2017>, 2017.
- 664 Barrie, L. A., Yi, Y., Leaitch, W. R., Lohmann, U., Kasibhatla, P., Roelofs, G. J., Wilson, J., McGovern, F., Benkovitz, C.,
665 Mélières, M. A., Law, K., Prospero, J., Kritz, M., Bergmann, D., Bridgeman, C., Chin, M., Christensen, J., Easter,
666 R., Feichter, J., Land, C., Jeuken, A., Kjellström, E., Koch, D., and Rasch, P.: A comparison of large-scale
667 atmospheric sulphate aerosol models (COSAM): Overview and highlights, *Tellus B Chem Phys Meteorol*, 53, 615–
668 645, <https://doi.org/10.3402/tellusb.v53i5.16642>, 2001.
- 669 Bauer, S. E., Koch, D., Unger, N., Metzger, S. M., Shindell, D. T., and Streets, D. G.: Nitrate aerosols today and in 2030: a
670 global simulation including aerosols and tropospheric ozone, *Atmos. Chem. Phys.*, 7, 5043–5059,
671 <https://doi.org/10.5194/acp-7-5043-2007>, 2007.
- 672 Bauer, S. E., Tsigaridis, K., and Miller, R.: Significant atmospheric aerosol pollution caused by world food cultivation,
673 *Geophys. Res. Lett.*, 43, 5394–5400, doi:10.1002/2016GL068354, 2016.
- 674 Bauer, S.E., Tsigaridis, K., Faluvegi, G., Nazarenko, L., Miller, R.L., Kelley, M., and Schmidt, G.: The turning point of the
675 aerosol era. *J. Adv. Model. Earth Syst.*, 14, no. 12, e2022MS003070, doi:10.1029/2022MS003070, 2022.
- 676 Bellouin, N., Quaas, J., Gryspenert, E., Kinne, S., Stier, P., Watson-Parris, D., Boucher, O., Carslaw, K. S., Christensen, M.,
677 Daniau, A. L., Dufresne, J. L., Feingold, G., Fiedler, S., Forster, P., Gettelman, A., Haywood, J. M., Lohmann, U.,
678 Malavelle, F., Mauritzen, T., McCoy, D. T., Myhre, G., Mülmenstädt, J., Neubauer, D., Possner, A., Rugenstein,
679 M., Sato, Y., Schulz, M., Schwartz, S. E., Sourdeval, O., Storelvmo, T., Toll, V., Winker, D., and Stevens, B.:
680 Bounding Global Aerosol Radiative Forcing of Climate Change, <https://doi.org/10.1029/2019RG000660>, 1 March
681 2020.
- 682



- 683 Bergametti, G., Gomes, L., Doude-Gaussens, G., Rognon, P., and Le Coustumer, M. N: African dust observed over the
684 Canary Islands: source-regions identification and the transport pattern for some summer situations, *J Geophys Res*,
685 94, 14855–14864, 1989.
- 686 Bond, T., Doherty, S. J., Fahey, D., Forster, P., Bernsten, T., DeAngelo, B., Flanner, M., Ghan, S., Karcher, B., Koch, D.,
687 Kinne, S., Kondo, Y., Quinn, P. K., Sarofim, M., Schultz, M., Venkataraman, C., Zhang, H., Zhang, S., Bellouin,
688 N., Guttikunda, S., Hopke, P., Jacobson, M., Kaiser, J. W., Klimont, Z., Lohman, U., Schwartz, J., Shindel, D.,
689 Storelvmo, T., Warren, S., and Zender, C.: Bounding the role of black carbon in the climate system: A scientific
690 assessment, *J Geophys Res*, D118, 5380–5552; doi:10.1002/jgrd_50171, 2013.
- 691 Bond, T. C., Streets, D. G., Yarber, K. F., Nelson, S. M., Woo, J.-H., and Klimont, Z.: A technology-based global inventory
692 of black and organic carbon emissions from combustion, *J Geophys Res*, 109, doi:10.1029/2003JD003697, 2004.
- 693 Bouet, C., Labiad, M. T., Rajot, J. L., Bergametti, G., Marticorena, B., des Tureaux, T. H., Ltifi, M., Sekrafi, S., and Féron,
694 A.: Impact of desert dust on air quality: What is the meaningfulness of daily PM standards in regions close to the
695 sources? The example of Southern Tunisia, *Atmosphere (Basel)*, 10, <https://doi.org/10.3390/atmos10080452>, 2019.
- 696 Bowdalo, D., Basart, S., Guevara, M., Jorba, O., Pérez García-Pando, C., Palomera, M. J., Rivera Hernandez, O., Puchalski,
697 M., Gay, D., Klausen, J., Moreno, S., Netcheva, S., and Tarasova, O.: GHOST: A globally harmonised dataset of
698 surface atmospheric composition measurements, *Earth Syst Sci Data*, 1–37,
699 <https://doi.org/10.5281/zenodo.10637449>, 2024.
- 700 Bozlaker, A., Buzcu-Güven, B., Fraser, M. P., and Chellam, S.: Insights into PM10 sources in Houston, Texas: Role of
701 petroleum refineries in enriching lanthanoid metals during episodic emission events, *Atmos Environ*, 69, 109–117,
702 <https://doi.org/10.1016/j.atmosenv.2012.11.068>, 2013.
- 703 Brahney, J., Mahowald, N., Ward, D. S., Ballantyne, A. P., and Neff, J. C.: Is atmospheric phosphorus pollution altering
704 global alpine Lake stoichiometry?, *Global Biogeochem Cycles*, 29, 1369–1383,
705 <https://doi.org/10.1002/2015GB005137>, 2015.
- 706 Brodsky, H., Calderon, R., Hamilton, D. S., Li, L., Miles, A. D., Pavlick, R. P., Gold, K. M., Crandall, S. G., and Mahowald,
707 N. M.: Assessing long-distance atmospheric transport of soilborne plant pathogens, *Environmental Research
708 Letters*, <https://doi.org/10.1088/1748-9326/acf50c>, 2023.
- 709 Bullard, J., Baddock, M., McTainsh, G., and Leys, J.: Sub-basin scale dust source geomorphology detected using MODIS,
710 *Geophys Res Lett*, 35, <https://doi.org/10.1029/2008GL033928>, 2008.
- 711 Burnett, R., Chen, H., Szyszkowicz, M., Fann, N., Hubbell, B., Pope, C. A., Apte, J. S., Brauer, M., Cohen, A., Weichenthal,
712 S., Coggins, J., Di, Q., Brunekreef, B., Frostad, J., Lim, S. S., Kan, H., Walker, K. D., Thurston, G. D., Hayes, R.
713 B., Lim, C. C., Turner, M. C., Jerrett, M., Krewski, D., Gapstur, S. M., Diver, W. R., Ostro, B., Goldberg, D.,
714 Crouse, D. L., Martin, R. v., Peters, P., Pinault, L., Tjepkema, M., van Donkelaar, A., Villeneuve, P. J., Miller, A.
715 B., Yin, P., Zhou, M., Wang, L., Janssen, N. A. H., Marra, M., Atkinson, R. W., Tsang, H., Thach, T. Q., Cannon, J.
716 B., Allen, R. T., Hart, J. E., Laden, F., Cesaroni, G., Forastiere, F., Weinmayr, G., Jaensch, A., Nagel, G., Concin,



- 717 H., and Spadaro, J. v.: Global estimates of mortality associated with longterm exposure to outdoor fine particulate
718 matter, Proc Natl Acad Sci U S A, 115, 9592–9597, <https://doi.org/10.1073/pnas.1803222115>, 2018.
- 719 Burgos, M. A., E. Andrews, G. Titos, A. Benedetti, H. Bian, V. Buchard, G. Curci, Z. Kipling, A. Kirkevåg, H. Kokkola, A.
720 Laakso, J. Letertre-Danczak, M. T. Lund, H. Matsui, G. Myhre, C. Randles, M. Schulz, T. van Noije, K. Zhang, L.
721 Alados-Arboledas, U. Baltensperger, A. Jefferson, J. Sherman, J. Sun, E. Weingartner, and P. Zieger (2020), A
722 global model-measurement evaluation of particle light scattering coefficients at elevated relative humidity,
723 Atmospheric Chemistry and Physics, 20, 10231-10258, doi:10.5194/acp-20-10231-2020.
- 724 Burrows, S. M., Elbert, W., Lawrence, M. G., and Poschl, U.: Bacteria in the global atmosphere--Part 1:Review and
725 synthesis of literature for different ecosystems, Atmos Chem Phys, 9, 9263–9280, 2009.
- 726 Burrows, S. M., Ogunro, O., Frossard, A. A., Russell, L. M., Rasch, P. J., and Elliott, S. M.: A physically based framework
727 for modeling the organic fractionation of sea spray aerosol from bubble film Langmuir equilibria, Atmos Chem
728 Phys, 14, 13601–13629, <https://doi.org/10.5194/acp-14-13601-2014>, 2014.
- 729 Caldwell, P. M., Mametjanov, A., Tang, Q., van Rockel, L. P., Golaz, J. C., Lin, W., Bader, D. C., Keen, N. D., Feng, Y.,
730 Jacob, R., Maltrud, M. E., Roberts, A. F., Taylor, M. A., Veneziani, M., Wang, H., Wolfe, J. D., Balaguru, K.,
731 Cameron-Smith, P., Dong, L., Klein, S. A., Leung, L. R., Li, H. Y., Li, Q., Liu, X., Neale, R. B., Pinheiro, M., Qian,
732 Y., Ullrich, P. A., Xie, S., Yang, Y., Zhang, K., and Zhou, T.: The DOE E3SM Coupled Model Version
733 1: Description and Results at High Resolution, J Adv Model Earth Syst, <https://doi.org/10.1029/2019MS001870>,
734 2019.
- 735 Carslaw, K. S., Lee, L., Reddington, C., Pringle, K., Rap, A., Forster, P., Mann, G., Spracklen, D., Woodhouse, M., Regayre,
736 L., and Pierce, J.: Large contribution of natural aerosols to uncertainty in indirect forcing, Nature, 503, 67–71, 2013.
- 737 Chatziparaschos, M., Daskalakis, N., Myriokefalitakis, S., Kalivitis, N., Nenes, A., Gonçalves Ageitos, M., Costa-Surós, M.,
738 Pérez García-Pando, C., Zanoli, M., Vrekoussis, M., and Kanakidou, M.: Role of K-feldspar and quartz in global
739 ice nucleation by mineral dust in mixed-phase clouds, Atmos. Chem. Phys., 23, 1785–1801,
740 <https://doi.org/10.5194/acp-23-1785-2023>, 2023.
- 741 Chen, Y., Street, J., and Paytan, A.: Comparison between pure-water- and seawater-soluble nutrient concentrations of
742 aerosol particles from the {Gulf} of {Aqaba}, Mar Chem, 101, 141–152,
743 <https://doi.org/10.1016/j.marchem.2006.02.002>, 2006.
- 744 Chuang, P., Duvall, R., Shafer, M., and Schauer, J.: The origin of water soluble particulate iron in the Asian atmospheric
745 outflow, Geophys Res Lett, 32, doi:10.1029/2004GL021946, 2005.
- 746 Cipoli, Y. A., Alves, C., Rapuano, M., Evtyugina, M., Rienda, I. C., Kováts, N., Vicente, A., Giardi, F., Furst, L., Nunes, T.,
747 and Feliciano, M.: Nighttime–daytime PM10 source apportionment and toxicity in a remoteness inland city of the
748 Iberian Peninsula, Atmos Environ, 303, <https://doi.org/10.1016/j.atmosenv.2023.119771>, 2023.
- 749 Clark, S. K., Ward, D. S., and Mahowald, N. M.: The sensitivity of global climate to the episodicity of fire aerosol emissions,
750 Journal of Geophysical Research: Atmospheres, 120, <https://doi.org/10.1002/2015JD024068>, 2015.



- 751 Cohen, D., Garton, D., Stelcer, E., Hawas, O., Wang, T., Pon, S., Kim, J., Choi, B., Oh, S., Shin, H.-J., Ko, M., and
752 Uematsu, M.: Multielemental analysis and characterization of fine aerosols at several key ACE-Asia sites, 109,
753 doi:10.1029/2003JD003569, 2004.
- 754 Collaud Coen, M., Andrews, E., Lastuey, A., Petkov Arsov, T., Backman, J., Brem, B. T., Bukowiecki, N., Couret, C.,
755 Eleftheriadis, K., Flentje, H., Fiebig, M., Gysel-Beer, M., Hand, J. L., Hoffer, A., Hooda, R., Hueglin, C., Joubert,
756 W., Keywood, M., Eun Kim, J., Kim, S. W., Labuschagne, C., Lin, N. H., Lin, Y., Lund Myhre, C., Luoma, K.,
757 Lyamani, H., Marinoni, A., Mayol-Bracero, O. L., Mihalopoulos, N., Pandolfi, M., Prats, N., Prenni, A. J., Putaud,
758 J. P., Ries, L., Reisen, F., Sellegri, K., Sharma, S., Sheridan, P., Patrick Sherman, J., Sun, J., Titos, G., Torres, E.,
759 Tuch, T., Weller, R., Wiedensohler, A., Zieger, P., and Laj, P.: Multidecadal trend analysis of in situ aerosol
760 radiative properties around the world, *Atmos Chem Phys*, 20, 8867–8908, <https://doi.org/10.5194/acp-20-8867-2020>, 2020.
- 761 Computational and Information Systems Laboratory: Cheyenne: HPE/SGI ICE XA System (NCAR Community
762 Computing), <https://doi.org/10.5065/D6RX99HX>, 2019.
- 763 da Silva, L. I. D., de Souza Sarkis, J. E., Zotin, F. M. Z., Carneiro, M. C., Neto, A. A., da Silva, A. dos S. A. G., Cardoso, M.
764 J. B., and Monteiro, M. I. C.: Traffic and catalytic converter - Related atmospheric contamination in the
765 metropolitan region of the city of Rio de Janeiro, Brazil, *Chemosphere*, 71, 677–684,
766 <https://doi.org/10.1016/j.chemosphere.2007.10.057>, 2008.
- 767 Dentener, F. J., Carmichael, G. R., Zhang, Y., Lelieveld, J., and Crutzen, P. J.: Role of mineral aerosol as a reactive surface
768 in the global troposphere, *J Geophys Res*, 101, 22,822-869,889, 1996.
- 769 Dentener, F., Kinne, S., Bond, T., Boucher, O., Cofala, J., Generoso, S., Ginoux, P., Gong, S., Hoelzemann, J. J., Ito, A.,
770 Marelli, L., Penner, J., Putaud, J.-P., Textor, C., Schulz, M., van der Werf, G. R., and Wilson, J.: Emissions of
771 primary aerosol and precursor gases in the years 2000 and 1750: prescribed data-sets for AeroCom, *Atmos Chem
772 Phys*, 6, 4321–4344, 2006.
- 773 Despres, V., Huffman, J., Burrows, S. M., Hoose, C., Safatov, A., Buryak, G., Frohlich-Nowoisky, J., Elbert, W., Andreae,
774 M., Polsch, U., and Jaenicke, R.: Primary biological aerosol particles in the atmosphere: a review, *Tellus B*, 64,
775 doi:10.3402/tellusb.v64i0.15598, 2012.
- 776 Dongarrà, G., Manno, E., Varrica, D., and Vultaggio, M.: Mass levels, crustal component and trace elements in PM10 in
777 Palermo, Italy, *Atmos Environ*, 41, 7977–7986, <https://doi.org/10.1016/j.atmosenv.2007.09.015>, 2007.
- 778 Dongarrà, G., Manno, E., Varrica, D., Lombardo, M., and Vultaggio, M.: Study on ambient concentrations of PM10, PM10-
779 2.5, PM2.5 and gaseous pollutants. Trace elements and chemical speciation of atmospheric particulates, *Atmos
780 Environ*, 44, 5244–5257, <https://doi.org/10.1016/j.atmosenv.2010.08.041>, 2010.
- 781 Dubovik, O., Smirnov, A., Holben, B. N., King, M. D., Kaufman, Y. J., ECK, T. F., and Slutsker, I.: Accuracy assessments of
782 aerosol optical properties retrieved from Aerosol Robotic Network (AERONET) Sun and sky radiance measurements,
783 *J Geophys Res*, 105, 9791–9806, 2000.



- 785 Dubovik, O., Holben, B., Eck, T. F., Smirnov, A., et al.: Variability of absorption and optical properties of key aerosol types
786 observed in worldwide locations, *Journal of Atmospheric Science*, 590–608, 2002.
- 787 Duce, R. A., Prospero, J. M., Chen, L., Merrill, J. T., and McDonald, R. L.: Transport of Mineral Aerosol From Asia Over
788 the North Pacific Ocean, *J Geophys Res*, 88, 5343–5352, 1983.
- 789 Engelbrecht, Johann, Eric V. McDonald, John A. Gillies, R. K. M. Jayanty, Gary Casuccio & Alan W. Gertler (2009)
790 Characterizing Mineral Dusts and Other Aerosols from the Middle East, Part 1: Ambient Sampling, Inhalation
791 Toxicology, 21:4, 297-326, DOI: 10.1080/08958370802464273, 2009.
- 792 Fanourakis, G. S., Kanakidou, M., Nenes, A., Bauer, S. E., Bergman, T., Carslaw, K. S., Grini, A., Hamilton, D. S.,
793 Johnson, J. S., Karydis, V. A., Kirkevåg, A., Kodros, J. K., Lohmann, U., Luo, G., Makkonen, R., Matsui, H.,
794 Neubauer, D., Pierce, J. R., Schmale, J., Stier, P., Tsigaridis, K., Van Noije, T., Wang, H., Watson-Parris, D.,
795 Westervelt, D. M., Yang, Y., Yoshioka, M., Daskalakis, N., Decesari, S., Gysel-Beer, M., Kalivitis, N., Liu, X.,
796 Mahowald, N. M., Myriokefalitakis, S., Schrödner, R., Sfakianaki, M., Tsimpidi, A. P., Wu, M., and Yu, F.:
797 Evaluation of global simulations of aerosol particle and cloud condensation nuclei number, with implications for
798 cloud droplet formation, *Atmos Chem Phys*, 19, 8591–8617, <https://doi.org/10.5194/acp-19-8591-2019>, 2019.
- 799 Fasullo, J. T., Lamarque, J. F., Hannay, C., Rosenbloom, N., Tilmes, S., DeRepentigny, P., Jahn, A., and Deser, C.: Spurious
800 Late Historical-Era Warming in CESM2 Driven by Prescribed Biomass Burning Emissions,
801 <https://doi.org/10.1029/2021GL097420>, 28 January 2022.
- 802 Fiore, A. M., Milly, G. P., Hancock, S. E., Quiñones, L., Bowden, J. H., Helstrom, E., Lamarque, J. F., Schnell, J., West, J.
803 J., and Xu, Y.: Characterizing Changes in Eastern U.S. Pollution Events in a Warming World, *Journal of
804 Geophysical Research: Atmospheres*, 127, <https://doi.org/10.1029/2021JD035985>, 2022.
- 805 Formenti, P., Elbert, W., Maenhaut, W., Haywood, J., and Andreae, M. O.: Chemical composition of mineral dust aerosol
806 during the Saharan Dust Experiment (SHADE) airborne campaign in the Cape Verde region, September 2000, *J.
807 Geophys. Res.*, 108, 8576, doi:10.1029/2002JD002648, 2003.
- 808 Furu, E., Katona-Szabo, I., Angyal, A., Szoboszlai, Z., Török, Z., and Kertész, Z.: The effect of the tramway track construction
809 on the aerosol pollution in Debrecen, Hungary, in: *Nuclear Instruments and Methods in Physics Research, Section B:
810 Beam Interactions with Materials and Atoms*, 124–130, <https://doi.org/10.1016/j.nimb.2015.08.014>, 2015.
- 811 Furu, E., Angyal, A., Szoboszlai, Z., Papp, E., Török, Z., and Kertész, Z.: Characterization of Aerosol Pollution in Two
812 Hungarian Cities in Winter 2009–2010, *Atmosphere (Basel)*, 13, <https://doi.org/10.3390/atmos13040554>, 2022.
- 813 Fuzzi, S., Decesari, S., Facchini, M., Cavalli, F., Emblico, L., Mircea, M., Andreae, M., Trebs, I., Hoffer, A., Guyon, P.,
814 Artaxo, P., Rizzo, L., Lara, L., Pauliquevis, T., Maenhaut, W., et al.: Overview of the inorganic and organic
815 composition of size-segregated aerosol in Rondonia, Brazil from the biomass-burning period to the onset of the wet
816 season., *J Geophys Res*, 112, doi:10.1029/2005JD006741, 2007.



- 817 Gantt, B., Meskhidze, N., Facchini, M. C., Rinaldi, M., Ceburnis, D., and O'Dowd, C. D.: Wind speed dependent size-
818 resolved parameterization for the organic mass fraction of sea spray aerosol, *Atmos Chem Phys*, 11, 8777–8790,
819 <https://doi.org/10.5194/acp-11-8777-2011>, 2011.
- 820 García, M. I., Rodríguez, S., and Alastuey, A.: Impact of North America on the aerosol composition in the North Atlantic
821 free troposphere, *Atmos Chem Phys*, 17, 7387–7404, <https://doi.org/10.5194/acp-17-7387-2017>, 2017.
- 822 Gelaro, R., McCarty, W., Suárez, M. J., Todling, R., Molod, A., Takacs, L., Randles, C. A., Darmenov, A., Bosilovich, M.
823 G., and Reichle, R.: The modern-era retrospective analysis for research and applications, version 2 (MERRA-2), *J
824 Clim*, 30, 5419–5454, 2017.
- 825 Gianini, M. F. D., Gehrig, R., Fischer, A., Ulrich, A., Wichser, A., and Hueglin, C.: Chemical composition of PM10 in
826 Switzerland: An analysis for 2008/2009 and changes since 1998/1999, *Atmos Environ*, 54, 97–106,
827 <https://doi.org/10.1016/j.atmosenv.2012.02.037>, 2012a.
- 828 Gianini, M. F. D., Fischer, A., Gehrig, R., Ulrich, A., Wichser, A., Piot, C., Besombes, J. L., and Hueglin, C.: Comparative
829 source apportionment of PM10 in Switzerland for 2008/2009 and 1998/1999 by Positive Matrix Factorisation,
830 *Atmos Environ*, 54, 149–158, <https://doi.org/10.1016/j.atmosenv.2012.02.036>, 2012b.
- 831 Gidden, M. J., Riahi, K., Smith, S. J., Fujimori, S., Luderer, G., Kriegler, E., Van Vuuren, D. P., Van Den Berg, M., Feng,
832 L., Klein, D., Calvin, K., Doelman, J. C., Frank, S., Fricko, O., Harmsen, M., Hasegawa, T., Havlik, P., Hilaire, J.,
833 Hoesly, R., Horing, J., Popp, A., Stehfest, E., and Takahashi, K.: Global emissions pathways under different
834 socioeconomic scenarios for use in CMIP6: A dataset of harmonized emissions trajectories through the end of the
835 century, *Geosci Model Dev*, 12, 1443–1475, <https://doi.org/10.5194/gmd-12-1443-2019>, 2019.
- 836 Ginoux, P., Chin, M., Tegen, I., Prospero, J. M., Holben, B. N., Dubovik, O., and Lin, S.-J.: Sources and distribution of dust
837 aerosol particles with the GOCART model, *J Geophys Res*, 106, 20255–20273, 2001.
- 838 Ginoux, P., Prospero, J., Gill, T. E., Hsu, N. C., and Zhao, M.: Global scale attribution of anthropogenic and natural dust
839 sources and their emission rates based on MODIS deep blue aerosol products, *Reviews of Geophysics*, 50,
840 DOI:10.1029/2012RG000388, 2012.
- 841 Gliß, J., Mortier, A., Schulz, M., Andrews, E., Balkanski, Y., Bauer, S. E., Benedictow, A. M. K., Bian, H., Checa-Garcia,
842 R., Chin, M., Ginoux, P., Griesfeller, J. J., Heckel, A., Kipling, Z., Kirkevåg, A., Kokkola, H., Laj, P., Le Sager, P.,
843 Lund, T. M., Lund Myhre, C., Matsui, H., Myhre, G., Neubauer, D., Van Noije, T., North, P., Olivie, D. J. L.,
844 Rémy, S., Sogacheva, L., Takemura, T., Tsigaridis, K., and Tsyro, S. G.: AeroCom phase III multi-model
845 evaluation of the aerosol life cycle and optical properties using ground- And space-based remote sensing as well as
846 surface in situ observations, *Atmos Chem Phys*, 21, 87–128, <https://doi.org/10.5194/acp-21-87-2021>, 2021.
- 847 Golaz, J. C., Caldwell, P. M., van Roekel, L. P., Petersen, M. R., Tang, Q., Wolfe, J. D., Abeshu, G., Anantharaj, V., Asay-
848 Davis, X. S., Bader, D. C., Baldwin, S. A., Bisht, G., Bogenschutz, P. A., Branstetter, M., Brunke, M. A., Brus, S.
849 R., Burrows, S. M., Cameron-Smith, P. J., Donahue, A. S., Deakin, M., Easter, R. C., Evans, K. J., Feng, Y.,
850 Flanner, M., Foucar, J. G., Fyke, J. G., Griffin, B. M., Hannay, C., Harrop, B. E., Hoffman, M. J., Hunke, E. C.,



- 851 Jacob, R. L., Jacobsen, D. W., Jeffery, N., Jones, P. W., Keen, N. D., Klein, S. A., Larson, V. E., Leung, L. R., Li,
852 H. Y., Lin, W., Lipscomb, W. H., Ma, P. L., Mahajan, S., Maltrud, M. E., Mametjanov, A., McClean, J. L., McCoy,
853 R. B., Neale, R. B., Price, S. F., Qian, Y., Rasch, P. J., Reeves Eyre, J. E. J., Riley, W. J., Ringler, T. D., Roberts, A.
854 F., Roesler, E. L., Salinger, A. G., Shaheen, Z., Shi, X., Singh, B., Tang, J., Taylor, M. A., Thornton, P. E., Turner,
855 A. K., Veneziani, M., Wan, H., Wang, H., Wang, S., Williams, D. N., Wolfram, P. J., Worley, P. H., Xie, S., Yang,
856 Y., Yoon, J. H., Zelinka, M. D., Zender, C. S., Zeng, X., Zhang, C., Zhang, K., Zhang, Y., Zheng, X., Zhou, T., and
857 Zhu, Q.: The DOE E3SM Coupled Model Version 1: Overview and Evaluation at Standard Resolution, *J Adv
858 Model Earth Syst.*, 11, 2089–2129, <https://doi.org/10.1029/2018MS001603>, 2019.
- 859 Gonçalves Ageitos, M., Obiso, V., Miller, R. L., Jorba, O., Klose, M., Dawson, M., Balkanski, Y., Perlitz, J., Basart, S., Di
860 Tomaso, E., Escribano, J., Macchia, F., Montané, G., Mahowald, N., Green, R. O., Thompson, D. R., and Pérez
861 García-Pando, C.: Modeling dust mineralogical composition: sensitivity to soil mineralogy atlases and their
862 expected climate impacts. *Atmos. Chem. Phys.*, 23, no. 15, 8623–8657, doi:10.5194/acp-23-8623-2023, 2023.
- 863 Gong, S. L., Barrie, L. A., Prospero, J. M., Savoie, D. L., Ayers, G. P., Blanchet, J.-P., and Spacek, L.: Modeling sea-salt
864 aerosol particles in the atmosphere 2. Atmospheric concentrations and fluxes, *J Geophys Res*, 102, 3819–3830,
865 1997.
- 866 Gong, S. L., Zhang, X. Y., Zhao, T. L., McKendry, I. G., Jaffe, D. A., and Lu, N. M.: Characterization of soil dust aerosol in
867 China and its transport and distribution during 2001 ACE-Asia: 2. Model simulation and validation, *J Geophys Res*,
868 108, 4262, 2003.
- 869 Graham, B., Guyon, P., Maenhaut, W., Taylor, P. E., Ebert, M., Matthias-Maser, S., Mayol-Bracero, O. L., Godoi, R. H. M.,
870 Artaxo, P., Meixner, F. X., Moura, M. A. L., Rocha, C. H. E., Van Grieken, R., Globsky, M. M., Flagan, R. C., and
871 Andreae, M. O.: Composition and diurnal variability of the natural Amazonian aerosol, *J Geophys Res*, 108, 4765,
872 doi:10.1029/2003JD004049, 2003.
- 873 Gulev, S. K., Thorne, P. W., Ahn, J., Dentener, F. J., Domingues, C. M., Gerland, S., Gong, D., Kaufman, D. S., Nnamchi,
874 H. C., Quaas, J., Rivera, J. A., Sathyendranath, S., Smith, S. L., Trewin, B., von Schuckmann, K., and Vose, R. ,S.:
875 Chapter 2: Changing State of the Climate System., in: *Climate Change 2021: The Physical Science Basis*.
876 Contribution of Working Group I to the Sixth Assessment Report of the Intergovernmental Panel on Climate
877 Change, edited by: Masson-Delmotte, V. , Zhai, P., Pirani, A., Connors, S. L., Péan, C., Berger, S., Caud, N., Chen,
878 Y., Goldfarb, L., Gomis, M. I., Huang, M., Leitzell, K., Lonnoy, E., Matthews, J. B. R., Maycock, T. K.,
879 Waterfield, T., Yelekçi, O., Yu, R., and Zhou, B. Cambridge University Press, Cambridge, United Kingdom and
880 New York, NY, USA, 287–422, <https://doi.org/10.1017/9781009157896.004>, 2021.
- 881 Gupta, G., Venkat Ratnam, M., Madhavan, B. L., and Narayananmurthy, C. S.: Long-term trends in Aerosol Optical Depth
882 obtained across the globe using multi-satellite measurements, *Atmos Environ*, 273,
883 <https://doi.org/10.1016/j.atmosenv.2022.118953>, 2022.



- 884 Hand, J. L., Gill, T. E., and Schichtel, B. A.: Spatial and seasonal variability in fine mineral dust and coarse aerosol mass at
885 remote sites across the United States, *J Geophys Res*, 122, 3080–3097, <https://doi.org/10.1002/2016JD026290>,
886 2017.
- 887 Hand, J. L., Gill, T. E., and Schichtel, B. A.: Urban and rural coarse aerosol mass across the United States: Spatial and
888 seasonal variability and long-term trends, *Atmos Environ*, 218, 117025,
889 <https://doi.org/10.1016/j.atmosenv.2019.117025>, 2019.
- 890 Hansen, J. and Nazarenko, L.: Soot climate forcing via snow and ice albedos, *PNAS*, 101, 423–428,
891 doi/10.1073/pnas.ss37157100, 2004.
- 892 Heald, C. and Spracklen, D.: Atmospheric budget of primary biological aerosol particles from fungal sources, *Geophys Res
893 Lett*, 36, doi:10.1029/2009GL037493, 2009.
- 894 Heald, C., Ridley, D., Kreidenweis, S., and Drury, E.: Satellite observations cap the atmospheric organic aerosol budget,
895 *Geophys Res Lett*, 37, L24808; doi:10.1029/2010GL045095, 2010.
- 896 Heimburger, A., Losno, R., Triquet, S., Dulac, F., and Mahowald, N.: Direct measurement of atmospheric iron, cobalt and
897 aluminum-derived dust deposition at Kerguelen Islands, *Global Biogeochem Cycles*, 26,
898 doi:10.1029/2012GB004301, <https://doi.org/10.1029/2012GB004301>, 2012.
- 899 Herut, B. and Krom, M.: Atmospheric input of nutrients and dust to the SE Mediterranean, in: *The Impact of Desert Dust
900 Across the Mediterranean*, edited by: Guerzoni, S. and Chester, R., 349–360, 1996.
- 901 Herut, B., Nimmo, M., Medway, A., Chester, R., and Krom, M.D.: Dry atmospheric inputs of trace metals at the
902 Mediterranean coast of Israel (SE Mediterranean): sources and fluxes. *Atmos. Environ.*, 35, 803-813, 2001.
- 903 Hinds, W. C., *Aerosol Technology, Properties, Behavior and Measurement of Airborne Particles*, John Wiley, New York,
904 1999.
- 905 .Hsu, C. Y., Chiang, H. C., Lin, S. L., Chen, M. J., Lin, T. Y., and Chen, Y. C.: Elemental characterization and source
906 apportionment of PM10 and PM2.5 in the western coastal area of central Taiwan, *Science of the Total
907 Environment*, 541, 1139–1150, <https://doi.org/10.1016/j.scitotenv.2015.09.122>, 2016.
- 908 Huang, Y., Adebiyi, A. A., Formenti, P., and Kok, J. F.: Linking the Different Diameter Types of Aspherical Desert Dust
909 Indicates That Models Underestimate Coarse Dust Emission, *Geophys Res Lett*, 48,
910 <https://doi.org/10.1029/2020GL092054>, 2021.
- 911 Hueglin, C., Gehrig, R., Baltensperger, U., Gysel, M., Monn, C., and Vonmont, H.: Chemical characterisation of PM2.5,
912 PM10 and coarse particles at urban, near-city and rural sites in Switzerland, *Atmos Environ*, 39, 637–651,
913 <https://doi.org/10.1016/j.atmosenv.2004.10.027>, 2005.
- 914 Huneeus, N., Schulz, M., Balkanski, Y., Griesfeller, J., Prospero, J., Kinne, S., Bauer, S., Boucher, O., Chin, M., Dentener,
915 F., Diehl, T., Easter, R., Fillmore, D., Ghan, S., Ginoux, P., Grini, A., Horowitz, L., Koch, D., Krol, M. C.,
916 Landing, W., Liu, X., Mahowald, N., Miller, R., Morcrette, J.-J., Myhre, G., Penner, J., Perlitz, J., Stier, P.,



- 917 Takemura, T., and Zender, C. S.: Global dust model intercomparison in AeroCom phase i, *Atmos Chem Phys*, 11,
918 <https://doi.org/10.5194/acp-11-7781-2011>, 2011.
- 919 Hurrell, J. W., Holland, M. M., Gent, P. R., Ghan, S., Kay, J. E., Kushner, P. J., Lamarque, J.-F., Large, W. G., Lawrence,
920 D., Lindsay, K., Lipscomb, W. H., Long, M. C., Mahowald, N., Marsh, D. R., Neale, R. B., Rasch, P., Vavrus, S.,
921 Vertenstein, M., Bader, D., Collins, W. D., Hack, J. J., Kiehl, J., and Marshall, S.: The community earth system
922 model: A framework for collaborative research, *Bull Am Meteorol Soc*, 94, <https://doi.org/10.1175/BAMS-D-12-00121.1>, 2013.
- 923
- 924 IPCC: Summary for Policymakers, in: Climate Change 2021: The Physical Science Basis. Contribution of Working Group I
925 to the Sixth Assessment Report of the Intergovernmental Panel on Climate Change, edited by: Masson-Delmotte, V.
926 , P., Zhai, A., Pirani, S.L., Connors, C., Péan, S., Berger, N., Caud, Y., Chen, L., Goldfarb, M. I., Gomis, M.,
927 Huang, K., Leitzell, E., Lonnoy, J. B. R., Matthews, T. B. R., Maycock, T. K., Waterfield, T., Yelekçi, O., Yu, R.,
928 and Zhou B., Cambridge University Press, Cambridge, UK, 3–32, <https://doi.org/10.1017/9781009157896.001>,
929 2021.
- 930 Jaenicke, R.: Abundance of cellular material and proteins in the atmosphere, *Science* (1979), 308, 73,
931 <https://doi.org/10.1126/science.1106335>, 2005.
- 932 Janssen, R., Heald, C., Steiner, A., Perring, A., Huffman, J. A., Robinson, E., Twohy, C., and Ziembra, L.: Drivers of the
933 fungal spore bioaerosol budget: observational analysis and global modelling, *Atmos Chem Phys*, 1–36,
934 <https://doi.org/10.5194/acp-2020-569>, 2020.
- 935 Jensen, J. B. and Lee, S.: Giant sea-salt aerosols and warm rain formation in marine stratocumulus, *J Atmos Sci*, 65, 3678–
936 3694, <https://doi.org/10.1175/2008JAS2617.1>, 2008.
- 937 Kahn, R. A., Gaitley, B., Martonchik, J., Diner, D. J., Crean, K., and Holben, B.: MISR global aerosol optical depth
938 validation based on two years of coincident AERONET observations, *J Geophys Res*, 110,
939 doi:10.1029/2004JD004706, 2005.
- 940 Kalivitis, N., E. Gerasopoulos, M. Vrekoussis, G. Kouvarakis, N. Kubilay, N. Hatzianastassiou, I. Vardavas, and N.
941 Mihalopoulos (2007), Dust transport over the eastern Mediterranean derived from Total Ozone Mapping
942 Spectrometer, Aerosol Robotic Network, and surface measurements, *J. Geophys. Res.*, 112, D03202,
943 doi:10.1029/2006JD007510, 2007.
- 944 Kaly, F., Marticorena, B., Chatenet, B., Rajot, J. L., Janicot, S., Niang, A., Yahi, H., Thiria, S., Maman, A., Zakou, A.,
945 Coulibaly, B. S., Coulibaly, M., Koné, I., Traoré, S., Diallo, A., and Ndiaye, T.: Variability of mineral dust
946 concentrations over West Africa monitored by the Sahelian Dust Transect, *Atmos Res*, 164–165, 226–241,
947 <https://doi.org/10.1016/j.atmosres.2015.05.011>, 2015
- 948 Kanakidou, M., Seinfeld, J., Pandis, S., Barnes, I., Dentener, F., Facchini, M., et al.: Organic aerosol and global climate
949 modeling: a review, *Atmos Chem Phys*, 5, 1053–1123, 2005.



- 950 Kanakidou M., Myriokefalitakis S., Tsigaridis K.: Aerosols in atmospheric chemistry and biogeochemical cycles of
951 nutrients, Environ. Res. Lett. 13 063004, 2018. <https://doi.org/10.1088/1748-9326/aabcdb>
- 952 Karydis, V. A., Tsimpidi, A. P., Bacer, S., Pozzer, A., Nenes, A., and Lelieveld, J.: Global impact of mineral dust on cloud
953 droplet number concentration, Atmos. Chem. Phys., 17, 5601–5621, <https://doi.org/10.5194/acp-17-5601-2017>,
954 2017.
- 955 Klimont, Z., Kupiainen, K., Heyes, C., Purohit, P., Cofala, J., Rafaj, P., Borken-Kleefeld, J., and Schöpp, W.: Global
956 anthropogenic emissions of particulate matter including black carbon, Atmos Chem Phys, 17, 8681–8723,
957 <https://doi.org/10.5194/acp-17-8681-2017>, 2017.
- 958 Koch, D., Schulz, M., Kinne, S., McNaughton, C., et al.: Evaluation of black carbon estimations in global aerosol models,
959 Atmos Chem Phys, 9, 9001–9026, 2009.
- 960 Kok, J. F., Mahowald, N. M., Fratini, G., Gillies, J. A., Ishizuka, M., Leys, J. F., Mikami, M., Park, M.-S., Park, S.-U., van
961 Pelt, R. S., and Zobeck, T. M.: An improved dust emission model - Part 1: Model description and comparison
962 against measurements, Atmos Chem Phys, 14, <https://doi.org/10.5194/acp-14-13023-2014>, 2014a.
- 963 Kok, J. F., Albani, S., Mahowald, N. M., and Ward, D. S.: An improved dust emission model - Part 2: Evaluation in the
964 Community Earth System Model, with implications for the use of dust source functions, Atmos Chem Phys, 14,
965 <https://doi.org/10.5194/acp-14-13043-2014>, 2014b.
- 966 Kok, J. F., Ridley, D. A., Zhou, Q., Miller, R. L., Zhao, C., Heald, C. L., Ward, D. S., Albani, S., and Haustein, K.: Smaller
967 desert dust cooling effect estimated from analysis of dust size and abundance, Nat Geosci, 10, 274–278,
968 <https://doi.org/10.1038/ngeo2912>, 2017.
- 969 Kok, J. F., Adebiyi, A. A., Albani, S., Balkanski, Y., Checa-Garcia, R., Chin, M., Colarco, P. R., Hamilton, D. S., Huang, Y.,
970 Ito, A., Klose, M., Leung, D. M., Li, L., Mahowald, N. M., Miller, R. L., Obiso, V., Pérez García-Pando, C., Rocha-
971 Lima, A., Wan, J. S., and Whicker, C. A.: Improved representation of the global dust cycle using observational
972 constraints on dust properties and abundance, Atmos Chem Phys, 21, 8127–8167, <https://doi.org/10.5194/acp-21-8127-2021>, 2021.
- 974 Kok, J. F., Storelvmo, T., Karydis, V. A., Adebiyi, A. A., Mahowald, N. M., Evan, A. T., He, C., and Leung, D. M.: Mineral
975 dust aerosol impacts on global climate and climate change, <https://doi.org/10.1038/s43017-022-00379-5>, 2023.
- 976
- 977 Kubilay, N., Nickovic, S., Moulin, C., and Dulac, F.: An illustration of the transport and deposition of mineral dust onto the
978 eastern Mediterranean, Atmos Environ, 34, 1293–1303, 2000.
- 979 Kyllonen, K., Vestenius, M., Anttila, P., Makkonen, U., Aurela, M., Wängberg, I., Nerentorp Mastromonaco, M., and
980 Hakola, H.: Trends and source apportionment of atmospheric heavy metals at a subarctic site during 1996–2018,
981 Atmos Environ, 236, <https://doi.org/10.1016/j.atmosenv.2020.117644>, 2020.



- 982 Laing, J. R., Hopke, P. K., Hopke, E. F., Husain, L., Dutkiewicz, V. A., Paatero, J., and Viisanen, Y.: Long-term particle
983 measurements in finnish arctic: Part I - Chemical composition and trace metal solubility, *Atmos Environ*, 88, 275–
984 284, <https://doi.org/10.1016/j.atmosenv.2014.03.002>, 2014a.
- 985 Laing, J. R., Hopke, P. K., Hopke, E. F., Husain, L., Dutkiewicz, V. A., Paatero, J., and Viisanen, Y.: Long-term particle
986 measurements in finnish arctic: Part II - trend analysis and source location identification, *Atmos Environ*, 88, 285–
987 296, <https://doi.org/10.1016/j.atmosenv.2014.01.015>, 2014b.
- 988 Laj, P., Bigi, A., Rose, C., Andrews, E., Lund Myhre, C., Collaud Coen, M., Lin, Y., Wiedensohler, A., Schulz, M., A.
989 Ogren, J., Fiebig, M., Gliß, J., Mortier, A., Pandolfi, M., Petäja, T., Kim, S. W., Aas, W., Putaud, J. P., Mayol-
990 Bracero, O., Keywood, M., Labrador, L., Aalto, P., Ahlberg, E., Alados Arboledas, L., Alastuey, A., Andrade, M.,
991 Artinano, B., Ausmeel, S., Arsov, T., Asmi, E., Backman, J., Baltensperger, U., Bastian, S., Bath, O., Paul Beukes,
992 J., T. Brem, B., Bukowiecki, N., Conil, S., Couret, C., Day, D., Dayantolis, W., Degorska, A., Eleftheriadis, K.,
993 Fetfatzis, P., Favez, O., Flentje, H., I. Gini, M., Gregorić, A., Gysel-Beer, M., Gannet Hallar, A., Hand, J., Hoffer,
994 A., Hueglin, C., K. Hooda, R., Hyvärinen, A., Kalapov, I., Kalivitis, N., Kasper-Giebl, A., Eun Kim, J., Kouvarakis,
995 G., Kranjc, I., Krejci, R., Kulmala, M., Labuschagne, C., Lee, H. J., Lihavainen, H., Lin, N. H., Löschau, G.,
996 Luoma, K., Marinoni, A., Martins Dos Santos, S., Meinhardt, F., Merkel, M., Metzger, J. M., Mihalopoulos, N.,
997 Anh Nguyen, N., Ondracek, J., Pérez, N., Rita Perrone, M., Pichon, J. M., Picard, D., Pichon, J. M., Pont, V., Prats,
998 N., Prenni, A., Reisen, F., Romano, S., Sellegri, K., Sharma, S., Schauer, G., Sheridan, P., Patrick Sherman, J.,
999 Schütze, M., Schwerin, A., Sohmer, R., Sorribas, M., Steinbacher, M., Sun, J., Titos, G., et al.: A global analysis of
1000 climate-relevant aerosol properties retrieved from the network of Global Atmosphere Watch (GAW) near-surface
1001 observatories, *Atmos Meas Tech*, 13, 4353–4392, <https://doi.org/10.5194/amt-13-4353-2020>, 2020.
- 1002 Li, J., Carlson, B. E., Yung, Y. L., Lv, D., Hansen, J., Penner, J. E., Liao, H., Ramaswamy, V., Kahn, R. A., Zhang, P.,
1003 Dubovik, O., Ding, A., Lacis, A. A., Zhang, L., and Dong, Y.: Scattering and absorbing aerosols in the climate
1004 system, <https://doi.org/10.1038/s43017-022-00296-7>, 1 June 2022a.
- 1005 Li, L., Mahowald, N. M., Miller, R. L., Pérez Garcíá-Pando, C., Klose, M., Hamilton, D. S., Gonçalves Ageitos, M., Ginoux,
1006 P., Balkanski, Y., Green, R. O., Kalashnikova, O., Kok, J. F., Obiso, V., Paynter, D., and Thompson, D. R.:
1007 Quantifying the range of the dust direct radiative effect due to source mineralogy uncertainty, *Atmos Chem Phys*,
1008 21, 3973–4005, <https://doi.org/10.5194/acp-21-3973-2021>, 2021.
- 1009 Li, L., Mahowald, N. M., Kok, J. F., Liu, X., Wu, M., Leung, D. M., Hamilton, D. S., Emmons, L. K., Huang, Y., Meng, J.,
1010 Sexton, N., and Wan, J.: Importance of different parameterization changes for the updated dust cycle modelling in
1011 the Community Atmosphere Model (version 6.1), *Geoscientific Model Development Discussion*,
1012 <https://doi.org/10.5194/gmd-2022-31>, 2022b.
- 1013 Lim, S. S., Vos, T., Flaxman, A. D., Danaei, G., Shibuya, K., Adair-Rohani, H., and AlMazroa, M.; A comparative risk
1014 assessment of burden of disease and injury attributable to 67 risk factors and risk factor clusters in 21 regions,
1015 1990–2010: A systematic analysis for the Global Burden of Disease Study 2010., *Lancet*, 380, 2224–2260, 2012.



- 1016 Liu, X., REaster, R. C., Ghan, S. J., Zaveri, R., Rasch, P., Shi, X., Lamarque, J.-F., Gettelman, A., Morrison, H., Vitt, F.,
1017 Conley, A., Park, S., Neale, R., Hannay, C., Ekman, A., Hess, P., Mahowald, N., Collins, W., Iacono, M.,
1018 Bretherton, C., Flanner, M., and Mitchell, D.: Toward a minimal representation of aerosols in climate models:
1019 Description and evaluation in the Community Atmosphere Model CAM5, Geoscientific Model Development, 5,
1020 709–739, doi:10.5194/gmd-5-709-2012, 2012.
1021 Liu, X., Ma, P. L., Wang, H., Tilmes, S., Singh, B., Easter, R. C., Ghan, S. J., and Rasch, P. J.: Description and evaluation of
1022 a new four-mode version of the Modal Aerosol Module (MAM4) within version 5.3 of the Community Atmosphere
1023 Model, Geosci Model Dev, 9, 505–522, <https://doi.org/10.5194/gmd-9-505-2016>, 2016.
1024 Lucarelli, F., Calzolai, G., Chiari, M., Giannoni, M., Mochi, D., Nava, S., and Carraresi, L.: The upgraded external-beam
1025 PIXE/PIGE set-up at LABEC for very fast measurements on aerosol samples, Nucl Instrum Methods Phys Res B,
1026 318, 55–59, <https://doi.org/10.1016/j.nimb.2013.05.099>, 2014.
1027 Lucarelli, F., Barrera, V., Becagli, S., Chiari, M., Giannoni, M., Nava, S., Traversi, R., and Calzolai, G.: Combined use of
1028 daily and hourly data sets for the source apportionment of particulate matter near a waste incinerator plant,
1029 Environmental Pollution, 247, 802–811, <https://doi.org/10.1016/j.envpol.2018.11.107>, 2019.
1030 Luo, C., Mahowald, N. M., and del Corral, J.: Sensitivity study of meteorological parameters on mineral aerosol mobilization,
1031 transport, and distribution, Journal of Geophysical Research D: Atmospheres, 108, 2003.
1032 Luo, J., Han, Y., Zhao, Y., Liu, X., Huang, Y., Wang, L., Chen, K., Tao, S., Liu, J., and Ma, J.: An inter-comparative evaluation
1033 of PKU-FUEL global SO₂ emission inventory, Science of the Total Environment, 722,
1034 <https://doi.org/10.1016/j.scitotenv.2020.137755>, 2020.
1035 Mackey, K. R. M., Hunter, D., Fischer, E. V., Jiang, Y., Allen, B., Chen, Y., Liston, A., Reuter, J., Schladow, G., and Paytan,
1036 A.: Aerosol-nutrient-induced picoplankton growth in Lake Tahoe, J Geophys Res Biogeosci, 118, 1054–1067,
1037 <https://doi.org/10.1002/jgrg.20084>, 2013.
1038 Maenhaut, W., Cafmeyer, J., Ptasinski, J., Andreae, M. O., Andreae, T. W., Elbert, W., Meixner, F. X., Karnieli, A., and
1039 Ichoku, C.: Chemical composition and light scattering of the atmospheric aerosol at a remote site in the Negev
1040 desert, Israel, J. Aerosol Sci., 28 (suppl.), 73–74, 1997b.
1041 Maenhaut, W. and Cafmeyer, J.: Long-Term Atmospheric Aerosol Study at Urban and Rural Sites in Belgium Using Multi-
1042 Elemental Analysis by Particle-Induced X-Ray Emission Spectrometry and Short-Irradiation Instrumental Neutron
1043 Activation Analysis, X-Ray Spectrometry, 27, 236–246, [https://doi.org/10.1002/\(SICI\)1097-4539\(199807/08\)27:4<236::AID-XRS292>3.0.CO;2-F](https://doi.org/10.1002/(SICI)1097-4539(199807/08)27:4<236::AID-XRS292>3.0.CO;2-F), 1998.
1045 Maenhaut, W., Salomonovic, R., Cafmeyer, J., Ichoku, C., Karnieli, A., and Andreae, M. O.: Anthropogenic and natural
1046 radiatively active aerosol types at Sede Boker, Israel, J. Aerosol Sci., 27 (suppl., 47–48,
1047 [https://doi.org/10.1016/0021-8502\(96\)00096-1](https://doi.org/10.1016/0021-8502(96)00096-1), 1996a.
1048 Maenhaut, W., Koppen, G., and Artaxo, P.: Long-term atmospheric aerosol study in Cuiaba', Brazil: Multielemental
1049 composition, sources, and impact of biomass burning, in: Biomass Burning and Global Change, vol. 2, Biomass



- 1050 Burning in South America, Southeast Asia, and Temperate and Boreal Ecosystems, and the Oil Fires of Kuwait,
1051 edited by: Levine, J. S., MIT Press, Cambridge Massachusetts, 637–652, 1996b.
- 1052 Maenhaut, W., Salma, I., Cafmeyer, J., Annegard, H., and Andreae, M.: Regional atmospheric aerosol composition and
1053 sources in the eastern Transvaal, South Africa and impact of biomass burning, *J Geophys Res*, 101, 23631–23650,
1054 1996c.
- 1055 Maenhaut, W., Francois, F., Cafmeyer, J., Gilot, C., and Hanssen, J. E.: Long-term aerosol study in southern Norway, and
1056 the relationship of aerosol components to source, in: *Proceedings of EUROTRAC Symposium '96*, vol. 1, Clouds,
1057 Aerosols, Modelling and Photo-oxidants, edited by: Borrell, P. M., Comput. Mech. Publ., South Hampton, UK),
1058 277–280, 1997a.
- 1059 Maenhaut, W., Fernandez-Jimenez, M.-T., and Artaxo, P.: Long-term study of atmospheric aerosols in Cuiaba, Brazil:
1060 Multielemental composition, sources and source apportionment, *J. Aerosol Sci.*, 30 (suppl., 259–260, 1999.
- 1061 Maenhaut, W., Fernandez-Jimenez, M.-T., Vanderzalm, J. L., Hooper, B., Hooper, M. A., and Tapper, N. J.: Aerosol
1062 composition at Jabiru, Australia, and impact of biomass burning, *J. Aerosol Sci.*, 31 (suppl., 745–746,
1063 [https://doi.org/10.1016/S0021-8502\(00\)90755-9](https://doi.org/10.1016/S0021-8502(00)90755-9), 2000a.
- 1064 Maenhaut, W., Fernandez-Jimenez, M.-T., Rajta, I., Dubtsov, S., Meixner, F. X., Andreae, M. O., Torr, S., Hargrove, J. W.,
1065 Chimanga, P., and Mlambo, J.: Long-term aerosol composition measurements and source apportionment at
1066 Rukomechi, Zimbabwe, *J. Aerosol Sci.*, 31 (suppl., 228–229, [https://doi.org/10.1016/S0021-8502\(00\)90237-4.](https://doi.org/10.1016/S0021-8502(00)90237-4.),
1067 2000b.
- 1068 Maenhaut, W., De Ridder, D. J. A., Fernandez-Jimenez, M.-T., Hooper, M. A., Hooper, B., and Nurhayati, M.: Long-term
1069 observations of regional aerosol composition at two sites in Indonesia, *Nucl. Instrum. Methods Phys. Res., Sect. B.*,
1070 189, 259–265, [https://doi.org/10.1016/S0168- 583X\(01\)01054-0.](https://doi.org/10.1016/S0168- 583X(01)01054-0.), 2002a.
- 1071 Maenhaut, W., Fernandez-Jimenez, M.-T., Rajta, I., and Artaxo, P.: Two-year study of atmospheric aerosol particles in Alta
1072 Floresta, Brazil: Multielemental composition and source apportionment, *Nuclear Instruments and Methods in
1073 Physics Research B*, 189, 243–248, 2002b.
- 1074 Maenhaut, W., Raes, N., Chi, X., Cafmeyer, J., Wang, W., and Salma, I.: Chemical composition and mass closure for fine
1075 and coarse aerosols at a kerbside in Budapest, Hungary, in spring 2002, *X-Ray Spectrometry*, 34, 290–296,
1076 <https://doi.org/10.1002/xrs.820>, 2005.
- 1077 Maenhaut, W., Raes, N., Chi, X., Cafmeyer, J., and Wang, W.: Chemical composition and mass closure for PM2.5 and PM
1078 10 aerosols at K-puszta, Hungary, in summer 2006, in: *X-Ray Spectrometry*, 193–197,
1079 <https://doi.org/10.1002/xrs.1062>, 2008.
- 1080 Maenhaut, W., Nava, S., Lucarelli, F., Wang, W., Chi, X., and Kulmala, M.: Chemical composition, impact from biomass
1081 burning, and mass closure for PM2.5 and PM10 aerosols at Hyttiälä, Finland, in summer 2007, *X-Ray
1082 Spectrometry*, 40, 168–171, <https://doi.org/10.1002/xrs.1302>, 2011.



- 1083 Mahowald, N., Li, L., Vira, J., Prank, M., Hamilton, D. S., Matsui, H., Miller, R. L., Lu, L., Akyuz, E. A., Daphne, M., Hess,
1084 P., Lihavainen, H., Wiedinmyer, C., Hand, J., Alaimo, M. G., Alves, C., Alastuey, A., Artaxo, P., Barreto, A.,
1085 Barraza, F., Becagli, S., Calzolai, G., Chellam., S., Chen, Y., Chuang, P., Cohen, D. Colombi, C., Diapouli, E.
1086 Dongarra, G., Eleftheriadis, K., Galy-Lacaux, C., Gaston, C., Gomez, D., Gonzalez Ramos, Y., Hakola, H.,
1087 Harrison, R., Heyes, C., Herut, B., Hopke, P., Huglin, C., Kanakidou, M., Kertesz, Z., Klimont, Z., Kyllonen, K.,
1088 Lambert, F., Liu, X., Losno, R., Lucarelli, F., Maenhaut, W., Marticorena, B., Martin, R., Mihalopoulos, N.,
1089 Morera-Gomez, Y. Paytan, A., Prospero, J., Rodriguez, S., Smichowski, P., Varrica, D., Walsh, B. Weagle, C.,
1090 Zhao, X. (2024). Datasets for: AERO-MAP: A data compilation and modelling approach to understand the fine and
1091 coarse mode aerosol composition (January 4, 2024 version) [Data set]. Zenodo.
<https://doi.org/10.5281/zenodo.10459654>
- 1092
- 1093 Mahowald, N., Artaxo, P., Baker, A., Jickells, T., Okin, G., Randerson, J., and Townsend, A.: Impact of biomass burning
1094 emissions and land use change on Amazonian atmospheric cycling and deposition of phosphorus, Global
1095 Biogeochem Cycles, 19, GB4030; 10.1029/2005GB002541, 2005.
- 1096 Mahowald, N., Lamarque, J.-F., Tie, X., and Wolff, E.: Sea salt aerosol response to climate change: last glacial maximum,
1097 pre-industrial, and doubled-carbon dioxide climates, J Geophys Res, 111, D05303; doi:10.1029/2005JD006459,
1098 2006.
- 1099 Mahowald, N., Jickells, T. D., Baker, A. R., Artaxo, P., Benitez-Nelson, C. R., Bergametti, G., Bond, T. C., Chen, Y.,
1100 Cohen, D. D., Herut, B., Kubilay, N., Losno, R., Luo, C., Maenhaut, W., McGee, K. A., Okin, G. S., Siefert, R. L.,
1101 and Tsukuda, S.: Global distribution of atmospheric phosphorus sources, concentrations and deposition rates, and
1102 anthropogenic impacts, Global Biogeochem Cycles, 22, <https://doi.org/10.1029/2008GB003240>, 2008.
- 1103 Mahowald, N., Ward, D. S., Kloster, S., Flanner, M. G., Heald, C. L., Heavens, N. G., Hess, P. G., Lamarque, J.-F., and
1104 Chuang, P. Y.: Aerosol Impacts on Climate and Biogeochemistry, Annu Rev Environ Resour, 36, 45–74,
1105 <https://doi.org/10.1146/annurev-environ-042009-094507>, 2011.
- 1106 Mahowald, N., Jickells, T. D., Baker, A. R., Artaxo, P., Benitez-Nelson, C. R., Bergametti, G., Bond, T. C., Chen, Y.,
1107 Cohen, D. D., Herut, B., Kubilay, N., Losno, R., Luo, C., Maenhaut, W., McGee, K. A., Okin, G. S., Siefert, R. L.,
1108 and Tsukuda, S.: Global distribution of atmospheric phosphorus sources, concentrations and deposition rates, and
1109 anthropogenic impacts, Global Biogeochem Cycles, 22, <https://doi.org/10.1029/2008GB003240>, 2008.
- 1110 Mahowald, N., Ward, D. S., Kloster, S., Flanner, M. G., Heald, C. L., Heavens, N. G., Hess, P. G., Lamarque, J.-F., and
1111 Chuang, P. Y.: Aerosol impacts on climate and biogeochemistry, Annu Rev Environ Resour, 36,
1112 <https://doi.org/10.1146/annurev-environ-042009-094507>, 2011.
- 1113 Mahowald, N. M., Engelstaedter, S., Luo, C., Sealy, A., Artaxo, P., Benitez-Nelson, C., Bonnet, S., Chen, Y., Chuang, P. Y.,
1114 Cohen, D., Dulac, F., Herut, B., Johansen, A. M., Kubilay, N., Losno, R., Maenhaut, W., Paytan, A., Prospero, J.
1115 M., Shank, L. M., and Siefert, R. L.: Atmospheric Iron Deposition: Global Distribution, Variability, and Human



- 1116 Perturbations, Annual Review of Marine Science of Marine Science, 1, 245–278,
1117 <https://doi.org/10.1146/annurev.marine.010908.163727>, 2009.
- 1118 Mahowald, N. M., Scanza, R., Brahney, J., Goodale, C. L., Hess, P. G., Moore, J. K., and Neff, J.: Aerosol Deposition
1119 Impacts on Land and Ocean Carbon Cycles, *Curr Clim Change Rep.* 3, 16–31, <https://doi.org/10.1007/s40641-017-0056-z>, 2017.
- 1120 Mahowald, N. M., Hamilton, D. S., Mackey, K. R. M., Moore, J. K., Baker, A. R., Scanza, R., and Zhang, Y.: Aerosol trace
1121 metal deposition dissolution and impacts on marine microorganisms and biogeochemistry, *Nature Communication*,
1122 81, 1–15, <https://doi.org/10.1038/s41467-018-04970-7>, 2018.
- 1123 Malm, W., Pitchford, M., McDade, C., and Ashbaugh, L.: Coarse particle speciation at selected locations in the rural
1124 continental United States, *Atmos Environ.* 41, 225–2239, 2007.
- 1125 Mbengue, S., Zikova, N., Schwarz, J., Vodička, P., Šmejkalová, A. H., and Holoubek, I.: Mass absorption cross-section and
1126 absorption enhancement from long term black and elemental carbon measurements: A rural background station in
1127 Central Europe, *Science of the Total Environment*, 794, <https://doi.org/10.1016/j.scitotenv.2021.148365>, 2021.
- 1128 Marticorena, B., Chatenet, B., Rajot, J., Traore, S., Diallo, A., Kone, I., Maman, A., NDiaye, T., and Zakou, A.: Temporal
1129 variability of mineral dust concentrations over West Africa: analyses of a pluriannual monitoring from the AMMA
1130 Sahelian Dust Transect, *Atmos. Chem. Phys.*, 10, 2010–8899, 2010.
- 1131 Matsui, H. and N. Mahowald (2017), Development of a global aerosol model using a two-dimensional sectional method: 2.
1132 Evaluation and sensitivity simulations, *Journal of Advances in Modeling Earth Systems*, 9, 1887–1920,
1133 doi:10.1002/2017MS000937.
- 1134 McNeill, J., Snider, G., Weagle, C. L., Walsh, B., Bissonnette, P., Stone, E., Abboud, I., Akoshile, C., Anh, N. X.,
1135 Balasubramanian, R., Brook, J. R., Coburn, C., Cohen, A., Dong, J., Gagnon, G., Garland, R. M., He, K., Holben,
1136 B. N., Kahn, R., Kim, J. S., Lagrosas, N., Lestari, P., Liu, Y., Jeba, F., Joy, K. S., Martins, J. V., Misra, A., Norford,
1137 L. K., Quel, E. J., Salam, A., Schichtel, B., Tripathi, S. N., Wang, C., Zhang, Q., Brauer, M., Gibson, M. D.,
1138 Rudich, Y., and Martin, R. V.: Large global variations in measured airborne metal concentrations driven by
1139 anthropogenic sources, *Sci Rep.* 10, <https://doi.org/10.1038/s41598-020-78789-y>, 2020.
- 1140 Mihalopoulos N., E. Stephanou, M. Kanakidou, S. Pilitsidis and P. Bousquet, Tropospheric aerosol ionic composition above
1141 the Eastern Mediterranean Area, *Tellus B*, 49B, 314–326, 1997.
- 1142 Mirante F., Oliveira C., Martins N., Pio C., Caseiro A., Cerqueira M., Alves C., Oliveira C., Oliveira J., Camões F., Matos
1143 M., and Silva H.: Carbonaceous content of atmospheric aerosols in Lisbon urban atmosphere. European
1144 Geophysical Union General Assembly, 2–7 May, Vienna, Austria, 2010.
- 1145 Mirante, F., Alves, C., Pio, C., Pindado, O., Perez, R., Revuelta, M. A., and Artiñano, B.: Organic composition of size
1146 segregated atmospheric particulate matter, during summer and winter sampling campaigns at representative sites in
1147 Madrid, Spain, *Atmos Res.* 132–133, 345–361, <https://doi.org/10.1016/j.atmosres.2013.07.005>, 2013.



- 1149 Mkoma, S. L.: Physico-chemical characterisation of atmospheric aerosols in Tanzania, with emphasis on the carbonaceous
1150 aerosol components and on chemical mass closure, Ghent University, Ghent, Belgium, 2008.
- 1151 Mkoma, S. L., Maenhaut, W., Chi, X., Wang, W., and Raes, N.: Characterisation of PM10 atmospheric aerosols for the wet
1152 season 2005 at two sites in East Africa, *Atmos Environ*, 43, 631–639,
1153 <https://doi.org/10.1016/j.atmosenv.2008.10.008>, 2009.
- 1154 Morera-Gómez, Y., Elustondo, D., Lasheras, E., Alonso-Hernández, C. M., and Santamaría, J. M.: Chemical characterization
1155 of PM10 samples collected simultaneously at a rural and an urban site in the Caribbean coast: Local and long-range
1156 source apportionment, *Atmos Environ*, 192, 182–192, <https://doi.org/10.1016/j.atmosenv.2018.08.058>, 2018.
- 1157 Morera-Gómez, Y., Santamaría, J. M., Elustondo, D., Lasheras, E., and Alonso-Hernández, C. M.: Determination and source
1158 apportionment of major and trace elements in atmospheric bulk deposition in a Caribbean rural area, *Atmos*
1159 *Environ*, 202, 93–104, <https://doi.org/10.1016/j.atmosenv.2019.01.019>, 2019.
- 1160 Mortier, A., Gliß, J., Schulz, M., Aas, W., Andrews, E., Bian, H., Chin, M., Ginoux, P., Hand, J., Holben, B., Zhang, H.,
1161 Kipling, Z., Kirkevåg, A., Laj, P., Lurton, T., Myhre, G., Neubauer, D., Olivié, D., von Salzen, K., Skeie, R. B.,
1162 Takemura, T., and Tilmes, S.: Evaluation of climate model aerosol trends with ground-based observations over the
1163 last 2 decades - an AeroCom and CMIP6 analysis, *Atmos Chem Phys*, 20, 13355–13378,
1164 <https://doi.org/10.5194/acp-20-13355-2020>, 2020.
- 1165 Myriokefalakis S., Nenes A., Baker A.R., Mihalopoulos N., Kanakidou M.: Bioavailable atmospheric phosphorous supply
1166 to the global ocean: a 3-D global modelling study, *Biogeosciences*, 13, 6519–6543, 2016,
1167 www.biogeosciences.net/13/6519/2016/
- 1168 Nava, S., Lucarelli, F., Amato, F., Becagli, S., Calzolai, G., Chiari, M., Giannoni, M., Traversi, R., and Udisti, R.: Biomass
1169 burning contributions estimated by synergistic coupling of daily and hourly aerosol composition records, *Science of*
1170 *the Total Environment*, 511, 11–20, <https://doi.org/10.1016/j.scitotenv.2014.11.034>, 2015.
- 1171 Nava, S., Calzolai, G., Chiari, M., Giannoni, M., Giardi, F., Becagli, S., Severi, M., Traversi, R., and Lucarelli, F.: Source
1172 apportionment of PM2.5 in Florence (Italy) by PMF analysis of aerosol composition records, *Atmosphere (Basel)*,
1173 11, <https://doi.org/10.3390/ATMOS11050484>, 2020.
- 1174 Neff, J., Reynolds, M. P., Munson, S., Fernandez, D., and Belnap, J.: The role of dust storms in total atmospheric particle
1175 concentration at two sites in the western U.S., *J Geophys Res*, 118, 1–12, 2013.
- 1176 Nenes, A., Pandis, S. N., Kanakidou, M., Russell, A., Song, S., Vasilakos, P., and Weber, R. J.: Aerosol acidity and liquid
1177 water content regulate the dry deposition of inorganic reactive nitrogen, *Atmos. Chem. Phys.*, 21, 6023–6033,
1178 <https://doi.org/10.5194/acp-21-6023-2021>, 2021.
- 1179 Nyanganyura, D., Maenhaut, W., Mathutu, M., Makarau, A., and Meixner, F. X.: The chemical composition of tropospheric
1180 aerosol particles and their contributing sources to a continental background site in northern Zimbabwe from 1994 to
1181 2000, *Atmos. Environ.*, 41, 2644–2659, <https://doi.org/10.1016/j.atmosenv.2006.11.015>, 2007.



- 1182 Obiso, V., Gonçalves Ageitos, M., Pérez García-Pando,C., Schuster, G. L., Bauer, S. E., Di Biagio, C., Formenti, P.
1183 Perlitz, J. P., Tsigaridis,K., and Miller, R. L., 2023: Observationally constrained regional variations of shortwave
1184 absorption by iron oxides emphasize the cooling effect of dust. *Atmos. Chem. Phys.*, submitted.
1185 Oliveira, C., Pio, C., Caseiro, A., Santos, P., Nunes, T., Mao, H., Luahana, L., and Sokhi, R.: Road traffic impact on urban
1186 atmospheric aerosol loading at Oporto, Portugal, *Atmos Environ.*, 44, 3147–3158,
1187 <https://doi.org/10.1016/j.atmosenv.2010.05.027>, 2010.
1188 Oliveira C., PAHLIS Team: Atmospheric pollution in Lisbon urban atmosphere. European Geosciences Union General
1189 Assembly, 19-24 Apr., Vienna, Austria, 2009.
1190 Olson, J., Prather, M., Berntsen, T., Carmichael, G., Chatfield, R., Connell, P., Derwent, R., Horowitz, L., Jin, S.,
1191 Kanakidou, M., Kasibhatla, P., Kotamarthi, R., Kuhn, M., Law, K., Penner, J., Perliski, L., Sillman, S., Stordal, F.,
1192 Thompson, A., and Wild, O.: Results from the Intergovernmental Panel on Climatic Change Photochemical Model
1193 Intercomparison (PhotoComp), *Journal of Geophysical Research: Atmospheres*, 102, 5979–5991,
1194 <https://doi.org/doi:10.1029/96JD03380>, 1997.
1195 Paulot, F., Ginoux, P., Cooke, W. F., Donner, L. J., Fan, S., Lin, M. Y., Mao, J., Naik, V., and Horowitz, L. W.: Sensitivity
1196 of nitrate aerosols to ammonia emissions and to nitrate chemistry: Implications for present and future nitrate optical
1197 depth, *Atmos Chem Phys*, 16, 1459–1477, <https://doi.org/10.5194/acp-16-1459-2016>, 2016.
1198 Pérez, N., Pey, J., Querol, X., Alastuey, A., López, J. M., and Viana, M.: Partitioning of major and trace components in
1199 PM10-PM2.5-PM1 at an urban site in Southern Europe, *Atmos Environ.*, 42, 1677–1691,
1200 <https://doi.org/10.1016/j.atmosenv.2007.11.034>, 2008.
1201 Philip, S., Martin, R. v., Snider, G., Weagle, C. L., van Donkelaar, A., Brauer, M., Henze, D. K., Klimont, Z.,
1202 Venkataraman, C., Guttikunda, S. K., and Zhang, Q.: Anthropogenic fugitive, combustion and industrial dust is a
1203 significant, underrepresented fine particulate matter source in global atmospheric models, *Environmental Research
1204 Letters*, 12, 1–46, 2017.
1205 Pio, C., Rienda, I. C., Nunes, T., Gonçalves, C., Tchepel, O., Pina, N. K., Rodrigues, J., Lucarelli, F., and Alves, C. A.:
1206 Impact of biomass burning and non-exhaust vehicle emissions on PM10 levels in a mid-size non-industrial western
1207 Iberian city, *Atmos Environ.*, 289, <https://doi.org/10.1016/j.atmosenv.2022.119293>, 2022.
1208 Prank, M., Sofiev, M., Tsyro, S., Hendriks, C., Semeena, V., Francis, X. V., Butler, T., Van Der Gon, H. D., Friedrich, R.,
1209 Hendricks, J., Kong, X., Lawrence, M., Righi, M., Samaras, Z., Sausen, R., Kukkonen, J., and Sokhi, R.: Evaluation
1210 of the performance of four chemical transport models in predicting the aerosol chemical composition in Europe in
1211 2005, *Atmos Chem Phys*, 16, 6041–6070, <https://doi.org/10.5194/acp-16-6041-2016>, 2016.
1212 Prospero, J., Bullard, J., and Hodkins, R.: High-Latitude Dust Over the North Atlantic: Inputs from Icelandic Proglacial Dust
1213 Storms, *Science* (1979), 335, 1078–1082, 2012.



- 1214 Prospero, J., Barkely, A., Gaston, C., Gatineau, A., Campos y Sanasano, A., and Pulcherie, K. P.: Data From: Characterizing
1215 and quantifying African dust transport and deposition to South America: Implications for the phosphorus budget in
1216 the Amazon Basin, Miami, <https://doi.org/10.17604/vrsh-w974>, 2020.
- 1217 Prospero, J. M.: Long-range transport of mineral dust in the global atmosphere: Impact of African dust on the environment
1218 of the southeastern United States, Proc. Natl. Academy Science, 96, 3396–3403, 1999.
- 1219 Prospero, J. M., Uematsu, M., and Savoie, D. L.: Mineral Aerosol Transport to the Pacific Ocean, in: Chemical
1220 Oceanography, vol. 10, Academic Press Limited, 187–218, 1989.
- 1221 Prospero, J.: The atmospheric transport of particles to the ocean, in: Particle Flux in the Ocean, edited by: Ittekkot, I.,
1222 Schaffer, P., Honjo, S., and Depetris, P. J., John Wiley, New York, 1996.
- 1223 Prospero, J. M., Barrett, K., Church, T., Dentener, F., Duce, R. A., Galloway, J. N., Levy, H., Moody, J., and Quinn, P.:
1224 Atmospheric deposition of nutrients to the North Atlantic Basin, Biogeochemistry, 35, 27–73,
1225 <https://doi.org/10.1007/BF02179824>, 1996.
- 1226 Putaud, J.-P., Raes, F., Dingenen, R. Van, U. Baltensperger, Bruggemann, E., Facchini, M.-C., Decesari, S., Fuzzi, S., R.
1227 Gehrig, Huglin, C., Laj, P., Lorbeer, G., Maenhaut, W., N. Mihalopoulos, Muller, K., Querol, X., Rodriguez, S.,
1228 Schneider, J., G. Spindler, ten Brink, H., Torseth, K., and Wiedensohler, A.: A European aerosol phenomenology.
1229 2: chemical characteristics of particulate matter at kerbside, urban, rural and background sites in Europe, Atmos
1230 Environ, 38, 2579–2595, 2004.
- 1231 Putaud, J. P., Van Dingenen, R., Alastuey, A., Bauer, H., Birmili, W., Cyrys, J., Flentje, H., Fuzzi, S., Gehrig, R., Hansson,
1232 H. C., Harrison, R. M., Herrmann, H., Hitzenberger, R., Hüglin, C., Jones, A. M., Kasper-Giebl, A., Kiss, G.,
1233 Kousa, A., Kuhlbusch, T. A. J., Löschau, G., Maenhaut, W., Molnar, A., Moreno, T., Pekkanen, J., Perrino, C., Pitz,
1234 M., Puxbaum, H., Querol, X., Rodriguez, S., Salma, I., Schwarz, J., Smolik, J., Schneider, J., Spindler, G., ten
1235 Brink, H., Tursic, J., Viana, M., Wiedensohler, A., and Raes, F.: A European aerosol phenomenology - 3: Physical
1236 and chemical characteristics of particulate matter from 60 rural, urban, and kerbside sites across Europe, Atmos
1237 Environ, 44, 1308–1320, <https://doi.org/10.1016/j.atmosenv.2009.12.011>, 2010.
- 1238 Quaas, J., Jia, H., Smith, C., Albright, A. L., Aas, W., Bellouin, N., Boucher, O., Doutriaux-Boucher, M., Forster, P. M.,
1239 Grosvenor, D., Jenkins, S., Klimont, Z., Loeb, N. G., Ma, X., Naik, V., Paulot, F., Stier, P., Wild, M., Myhre, G.,
1240 and Schulz, M.: Robust evidence for reversal of the trend in aerosol effective climate forcing, Atmos. Chem. Phys.,
1241 22, 12221–12239, <https://doi.org/10.5194/acp-22-12221-2022>, 2022.
- 1242 Regayre, L. A., Johnson, J. S., Yoshioka, M., Pringle, K. J., Sexton, D. M. H., Booth, B. B. B., Lee, L. A., Bellouin, N., and
1243 Carslaw, K. S.: Aerosol and physical atmosphere model parameters are both important sources of uncertainty in
1244 aerosol ERF, Atmos Chem Phys, 18, 9975–10006, <https://doi.org/10.5194/acp-18-9975-2018>, 2018.
- 1245 Reid, J. S., Jonson, H., Maring, H., Smirnov, A., Savoie, D., Cliff, S., Reid, E., Livingston, J., Meier, M., Dubovik, O., and
1246 Tsay, S.-C.: Comparison of size and morphological measurements of dust particles from Africa, J Geophys Res,
1247 108, 8593: doi:1029/2002JD002485, 2003.



- 1248 Remer, L., Kaufman, Y., Tanre, D., Mattoo, S., Chu, D., Martins, J., Li, R., Ichoku, C., Levy, R., Kleidman, R., Eck, T.,
1249 Vermote, E., and Holbren, B.: The MODIS aerosol algorithm, products and validation, *J Atmos Sci*, 62, 947–973,
1250 2005.
- 1251 Rodríguez, S., Alastuey, A., Alonso-Pérez, S., Querol, X., Cuevas, E., Abreu-Afonso, J., Viana, M., Pérez, N., Pandolfi, M.,
1252 and De La Rosa, J.: Transport of desert dust mixed with North African industrial pollutants in the subtropical
1253 Saharan Air Layer, *Atmos Chem Phys*, 11, 6663–6685, <https://doi.org/10.5194/acp-11-6663-2011>, 2011.
- 1254 Rodríguez, S., Alastuey, A., and Querol, X.: A review of methods for long term in situ characterization of aerosol dust,
1255 <https://doi.org/10.1016/j.aeolia.2012.07.004>, October 2012.
- 1256 Rodríguez, S., Cuevas, E., Prospero, J. M., Alastuey, A., Querol, X., López-Solano, J., García, M. I., and Alonso-Pérez, S.:
1257 Modulation of Saharan dust export by the North African dipole, *Atmos Chem Phys*, 15, 7471–7486,
1258 <https://doi.org/10.5194/acp-15-7471-2015>, 2015.
- 1259 Ryder, C. L., Highwood, E. J., Walser, A., Seibert, P., Philipp, A., and Weinzierl, B.: Coarse and giant particles are
1260 ubiquitous in Saharan dust export regions and are radiatively significant over the Sahara, *Atmos. Chem. Phys.*, 19,
1261 15353–15376, <https://doi.org/10.5194/acp-19-15353-2019>, 2019.
- 1262 Salma, I., Maenhaut, W., Annegarn, H. J., Andreae, M. O., Meixner, F. X., and Garstang, M.: Combined application of
1263 INAA and PIXE for studying the regional aerosol composition in Southern Africa, *Journal of Geophysical
1264 Research*, 101, 2361–23650, 1997.
- 1265 Savoie, D. L., Prospero, J. M., Larsen, R. J., Huang, R., Izaguirre, M. A., Huang, T., Snowdon, T., Custals, L., and
1266 Sanderson, C.: Nitrogen and sulfur species in Antarctic aerosols at Mawson, Palmer Station, and Marsh (King
1267 George Island), *J Atmos Chem*, 17, 95–122, 1993.
- 1268 Scanza, R., Mahowald, N., Ghan, S., Zender, C., Kok, J., Liu, X., and Zhang, Y.: Dependence of dust radiative forcing on
1269 mineralogy in the Community Atmosphere Model, *Atmos Chem Phys*, 15, 537–561, 2015.
- 1270 Schulz, M., Prospero, J. M., Baker, A. R., Dentener, F., Ickes, L., Liss, P. S., Mahowald, N. M., Nickovic, S., García-Pando,
1271 C. P., Rodríguez, S., Sarin, M., Tegen, I., and Duce, R. A.: Atmospheric transport and deposition of mineral dust to
1272 the ocean: Implications for research needs, *Environ Sci Technol*, 46, <https://doi.org/10.1021/es300073u>, 2012.
- 1273 Schuster, G. L., Dubovik, O., and Arola, A.: Remote sensing of soot carbon – Part 1: Distinguishing different absorbing
1274 aerosol species, *Atmos. Chem. Phys.*, 16, 1565–1585, <https://doi.org/10.5194/acp-16-1565-2016>, 2016.
- 1275 Schutgens, N. A. J., Gryspeerdt, E., Weigum, N., Tsyro, S., Goto, D., Schulz, M., and Stier, P.: Will a perfect model agree
1276 with perfect observations? The impact of spatial sampling, *Atmos Chem Phys*, 16, 6335–6353,
1277 <https://doi.org/10.5194/acp-16-6335-2016>, 2016.
- 1278 Seinfeld, J. H. and Pandis, S. N.: *Atmospheric Chemistry and Physics: From Air Pollution to Climate Change*, 2006.
- 1279 Silva, H.F., Matos, M. J., Oliveira, C., Ferreira, A. F., Oliveira, J. C., Cantinho, P., Calado, M., Oliveira, C., Martins, N., Pio,
1280 C., and Camões M. F. : Effect of climate on PM concentration and size distribution in two sites in the city of
1281 Lisbon, Encontro de Jovens Químicos Portugueses, Aveiro, 21 to 23 of April, 2010.



- 1282 Skiles, S. M. K., Flanner, M., Cook, J. M., Dumont, M., and Painter, T. H.: Radiative forcing by light-absorbing particles in
1283 snow, <https://doi.org/10.1038/s41558-018-0296-5>, 1 November 2018.
- 1284 Smichowski, P., Gómez, D. R., Dawidowski, L. E., Giné, M. F., Bellato, A. C. S., and Reich, S. L.: Monitoring trace metals
1285 in urban aerosols from Buenos Aires city. Determination by plasma-based techniques, *Journal of Environmental*
1286 *Monitoring*, 6, 286–294, <https://doi.org/10.1039/b312446k>, 2004.
- 1287 Smith, M. B., Mahowald, N. M., Albani, S., Perry, A., Losno, R., Qu, Z., Marticorena, B., Ridley, D. A., and Heald, C. L.:
1288 Sensitivity of the interannual variability of mineral aerosol simulations to meteorological forcing dataset, *Atmos*
1289 *Chem Phys*, 17, <https://doi.org/10.5194/acp-17-3253-2017>, 2017.
- 1290 Swap, R., Garstang, M., Greco, S., Talbot, R., and Kallberg, P.: Saharan dust in the Amazon Basin, *Tellus*, 44B, 133–149,
1291 <https://doi.org/https://doi.org/10.3402/tellusb.v44i2.15434>, 1992.
- 1292 Szopa, S., Naik, V., Adhikary, B., Artaxo, P., Berntsen, T., Collins, W. D., Aas, W., Akritidis, D., Allen, R. J., Kanaya, Y.,
1293 Prather, M. J., Kuo, C., Zhai, P., Pirani, A., Connors, S., Péan, C., Berger, S., Caud, N., Chen, Y., Goldfarb, L.,
1294 Gomis, M., Huang, M., Leitzell, K., Lonnoy, E., Matthews, J., Maycock, T., Waterfield, T., Yelekçi, O., Yu, R., and
1295 Zhou, B.: Chapter 6: Short-lived Climate Forcers, in: *Climate Change 2021: The Physical Science Basis*.
1296 Contribution of Working Group I to the Sixth Assessment Report of the Intergovernmental Panel on Climate
1297 Change, edited by: Masson-Delmotte, V. , Zhai, P., A. Pirani, A., Connors, S. L., Péan, C. S., Berger, S., Caud, N.,
1298 Chen, Y., Goldfarb, L., Gomis, M. I., Huang, M., Leitzell, K., Lonnoy, E., Matthews, J. B. R., Maycock, T. K.,
1299 Waterfield, T., Yelekçi, O., Yu, R., and Zhou, B., Cambridge University Press, , Cambridge, United Kingdom and
1300 New York, NY, USA, 816–921, <https://doi.org/10.1017/9781009157896.008>, 2021.
- 1301 Tanré, D., Kaufman, Y. J., Herman, M., and Mattoe, S.: Remote sensing of aerosol properties over oceans using the
1302 MODIS/EOS spectral radiances, *J Geophys Res*, 102, 16,916-971,988, 1997.
- 1303 Textor, C. and others: Analysis and quantification of the diversities of aerosol life cycles within AeroCOM, *Atmos Chem*
1304 *Phys*, 6, 1777–1813, 2006.
- 1305 Thornhill, G., Collins, W., Olivié, D., Archibald, A., Bauer, S., Checa-Garcia, R., Fiedler, S., Folberth, G., Gjermundsen, A.,
1306 Horowitz, L., Lamarque, J.-F., Michou, M., Mulcahy, J., Nabat, P., Naik, V., O'Connor, F., Paulot, F., Schulz, M.,
1307 Scott, C., Seferian, R., Smith, C., Takemura, T., Tilmes, S., and Weber, J.: Climate-driven chemistry and aerosol
1308 feedbacks in CMIP6 Earth system models, *Atmos Chem Phys*, 1–36, <https://doi.org/10.5194/acp-2019-1207>, 2020.
- 1309 Thornhill, G., Collins, W., Olivié, D., B. Skeie, R., Archibald, A., Bauer, S., Checa-Garcia, R., Fiedler, S., Folberth, G.,
1310 Gjermundsen, A., Horowitz, L., Lamarque, J. F., Michou, M., Mulcahy, J., Nabat, P., Naik, V., M. O'Connor, F.,
1311 Paulot, F., Schulz, M., E. Scott, C., Séférian, R., Smith, C., Takemura, T., Tilmes, S., Tsigaridis, K., and Weber, J.:
1312 Climate-driven chemistry and aerosol feedbacks in CMIP6 Earth system models, *Atmos Chem Phys*, 21, 1105–
1313 1126, <https://doi.org/10.5194/acp-21-1105-2021>, 2021.



- 1314 Toro, C., Sonntag, D., Bash, J., Burke, G., Murphy, B. N., Seltzer, K. M., Simon, H., Shephard, M. W., and Cady-Pereira, K.
1315 E.: Sensitivity of air quality to vehicle ammonia emissions in the United States, *Atmos Environ*, 327,
1316 <https://doi.org/10.1016/j.atmosenv.2024.120484>, 2024.
- 1317 Tørseth, K., Aas, W., Breivik, K., Fjeraa, A. M., Fiebig, M., Hjellbrekke, A. G., Lund Myhre, C., Solberg, S., and Yttri, K. E.:
1318 Introduction to the European Monitoring and Evaluation Programme (EMEP) and observed atmospheric composition
1319 change during 1972–2009, <https://doi.org/10.5194/acp-12-5447-2012>, 2012.
- 1320 Tsigaridis K., N. Daskalakis, M. Kanakidou, P. J. Adams, P. Artaxo, R. Bahadur, Y. Balkanski, S. E. Bauer, N. Bellouin, A.
1321 Benedetti, T. Bergman, T. K. Berntsen, J. P. Beukes, H. Bian, K. S. Carslaw, M. Chin, G. Curci, T. Diehl, R. C.
1322 Easter, S. J. Ghan, S. L. Gong, A. Hodzic, C. R. Hoyle, T. Iversen, S. Jathar, J. L. Jimenez, J. W. Kaiser, A. Kirkevag,
1323 D. Koch, H. Kokkola, Y. H Lee, G. Lin, X. Liu, G. Luo, X. Ma, G. W. Mann, N. Mihalopoulos, J.-J. Morcrette, J.-F.
1324 Muller, G. Myhre, S. Myrookefalitakis, N. L. Ng, D. O'Donnell, J. E. Penner, L. Pozzoli, K. J. Pringle, L. M. Russell,
1325 M. Schulz, J. Sciare, O. Seland, D. T. Shindell, S. Sillman, R. B. Skeie, D. Spracklen, T. Stavrakou, S. D. Steenrod,
1326 T. Takemura, P. Tiiitta, S. Tilmes, H. Tost, T. van Noije, P. G. van Zyl, K. von Salzen, F. Yu, Z. Wang, Z. Wang, R.
1327 A. Zaveri, H. Zhang, K. Zhang, Q. Zhang, and X. Zhang, The AeroCom evaluation and intercomparison of organic
1328 aerosol in global models, *Atmospheric Chemistry and Physics*, 14, pp. 10845–10895, 2014.
- 1329 Turnock, S. T., Allen, R. J., Andrews, M., Bauer, S. E., Deushi, M., Emmons, L., Good, P., Horowitz, L., John, J. G., Michou,
1330 M., Nabat, P., Naik, V., Neubauer, D., O'Connor, F. M., Olivie, D., Oshima, N., Schulz, M., Sellar, A., Shim, S.,
1331 Takemura, T., Tilmes, S., Tsigaridis, K., Wu, T., and Zhang, J.: Historical and future changes in air pollutants from
1332 CMIP6 models, *Atmos Chem Phys*, 20, 14547–14579, <https://doi.org/10.5194/acp-20-14547-2020>, 2020.
- 1333
- 1334 Van Donkelaar, A., Hammer, M. S., Bindle, L., Brauer, M., Brook, J. R., Garay, M. J., Hsu, N. C., Kalashnikova, O. V.,
1335 Kahn, R. A., Lee, C., Levy, R. C., Lyapustin, A., Sayer, A. M., and Martin, R. V.: Monthly Global Estimates of
1336 Fine Particulate Matter and Their Uncertainty, *Environ Sci Technol*, 55, 15287–15300,
1337 <https://doi.org/10.1021/acs.est.1c05309>, 2021.
- 1338 Vanderzalm, J. L., Hooper, M. A., Ryan, B., Maenhaut, W., P. Martin, P. R., Rayment, and Hooper, B. M.: Impact of
1339 seasonal biomass burning on air quality in the “Top End” of regional northern Australia, *Clean Air Environ.*
1340 Qual., 37, 28–34, 2003.
- 1341 Vet, R., Artz, R. S. R. S., Carou, S., Shaw, M., Ro, C.-U. C.-U., Aas, W., Baker, A., Bowersox, V. C., Dentener, F., Galy-
1342 Lacaux, C., Hou, A., Pienaar, J. J., Gillett, R., Forti, M. C. C., Gromov, S., Hara, H., Khodzher, T., Mahowald, N.
1343 M. N. M., Nickovic, S., Rao, P. S. P., Reid, N. W. N. W., Dentener, F., Galy-Lacaux, C., Hou, A., Gillett, R., Forti,
1344 M. C. C., Gromov, S., Hara, H., Khodzher, T., Mahowald, N. M. N. M., Nickovic, S., Reid, N. W. N. W., Vet, R.,
1345 Artz, R. S., Carou, S., Shaw, M., Ro, C.-U., Aas, W., Baker, A., Bowersox, V. C., Dentener, F., Galy-Lacaux, C.,
1346 Hou, A., Pienaar, J. J., Gillett, R., Forti, M. C., Gromov, S., Hara, H., Khodzher, T., Mahowald, N. M., Nickovic,
1347 S., Rao, P. S. P., and Reid, N. W. N. W.: A global assessment of precipitation chemistry and depositoin of sulfur,



- 1348 nitrogen, sea salt , base cations, organic acids, acidity and pH and phosphorus, Atmospheric Enviroment, 93, 3–100,
1349 2014.

1350 Vira, J., Hess, P., Melkonian, J., and Wieder, W. R.: An improved mechanistic model for ammonia volatilization in Earth
1351 system models: Flow of Agricultural Nitrogen version 2 (FANv2), Geosci Model Dev, 13, 4459–4490,
1352 <https://doi.org/10.5194/gmd-13-4459-2020>, 2020.

1353 Vira, J., Hess, P., Ossouhou, M., and Galy-Lacaux, C.: Evaluation of interactive and prescribed agricultural ammonia
1354 emissions for simulating atmospheric composition in CAM-chem, Atmos Chem Phys, 22, 1883–1904,
1355 <https://doi.org/10.5194/acp-22-1883-2022>, 2022.

1356 Virkkula, A., Aurela, M., Hillamo, R., Makela, T., Pakkanen, T., Kerminen, V. M., Maenhaut, W., Francois, F., and
1357 Cafmeyer, J.: Chemical composition of atmospheric aerosol in the European subarctic: Contribution of the Kola
1358 Peninsula smelter areas, central Europe and the Arctic Ocean, Journal Geophysical Research, 104, 23,681–23,696,
1359 <https://doi.org/10.1029/1999JD900426>, 1999.

1360 Watson-Parris, D., Bellouin, N., Deaconu, L. T., Schutgens, N. A. J., Yoshioka, M., Regayre, L. A., Pringle, K. J., Johnson,
1361 J. S., Smith, C. J., Carslaw, K. S., and Stier, P.: Constraining Uncertainty in Aerosol Direct Forcing, Geophys Res
1362 Lett, 47, <https://doi.org/10.1029/2020GL087141>, 2020.

1363 Webb, N. P. and Pierre, C.: Quantifying Anthropogenic Dust Emissions, Earths Future, 6, 286–295,
1364 <https://doi.org/10.1002/2017EF000766>, 2018.

1365 Wiedinmyer, C., Lihavainen, H., Mahowald, N., Alastuey, A., Albani, S., Artaxo, P., Bergametti, G., Batterman, S.,
1366 Brahney, J., Duce, R., Feng, Y., Buck, C., Ginoux, P., Chen, Y., Guieu, C., Cohen, D., Hand, J., Harrison, R.,
1367 Herut, B., and Zhang, Y.: COARSEMAP: synthesis of observations and models for coarse-mode aerosols, Fall
1368 American Geophysical Union, 2018.

1369 Wilson, W. E., Chow, J. C., Claiborn, C., Fusheng, W., Engelbrecht, J., and Watson, J. G.: Monitoring of particulate matter
1370 outdoors, 1009–1043 pp., 2002.

1371 Wolff, G. T.: Armoqheric Environment, 977–981 pp., 1984.

1372 Xiao, Y. H., Liu, S. R., Tong, F. C., Kuang, Y. W., Chen, B. F., and Guo, Y. D.: Characteristics and sources of metals in
1373 TSP and PM2.5 in an urban forest park at Guangzhou, Atmosphere (Basel), 5, 775–787,
1374 <https://doi.org/10.3390/atmos5040775>, 2014.

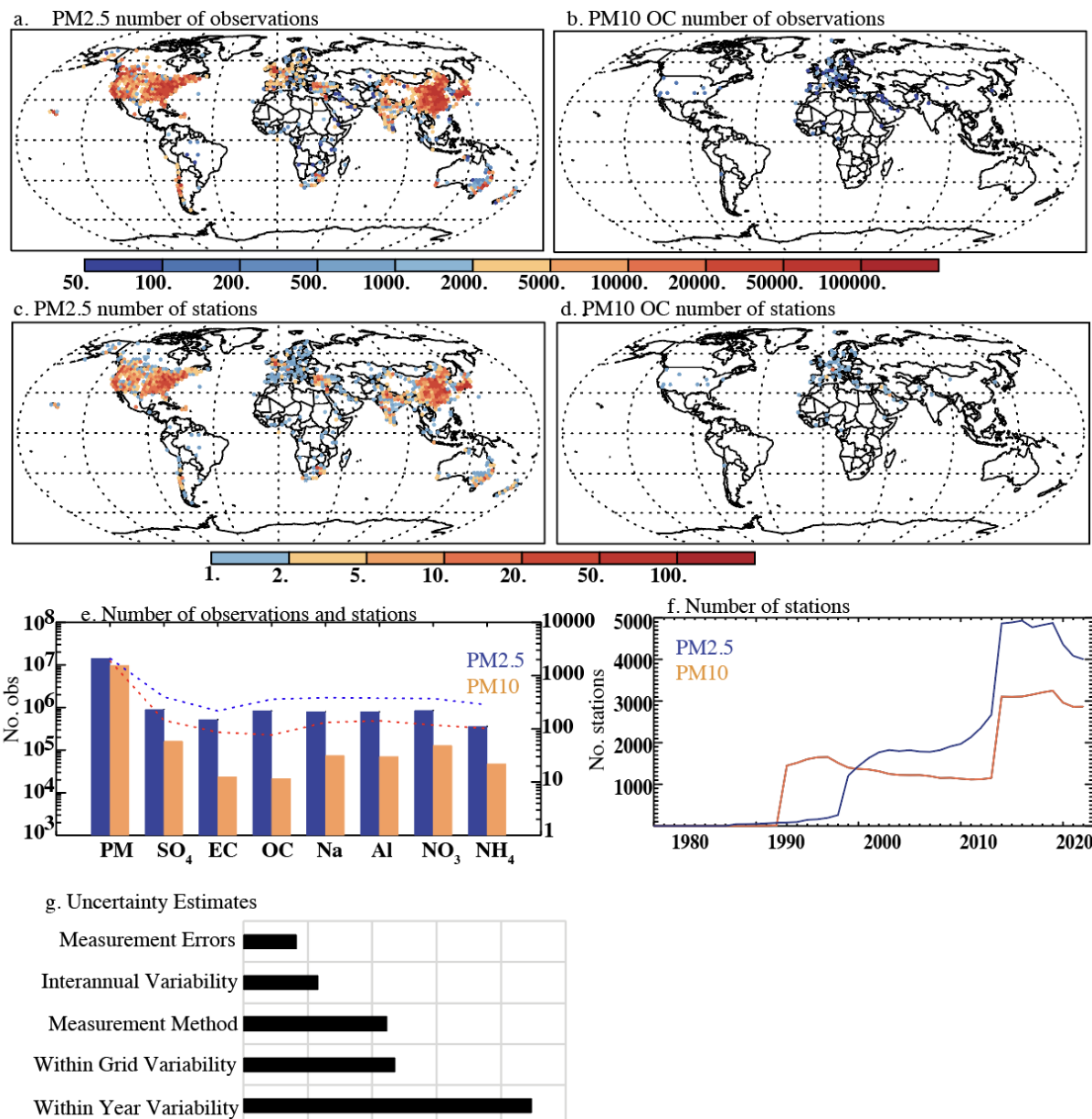
1375 Xu, L. and Penner, J. E.: Global simulations of nitrate and ammonium aerosols and their radiative effects, Atmos Chem
1376 Phys, 12, 9479–9504, <https://doi.org/10.5194/acp-12-9479-2012>, 2012.

1377 Yang, Y., Wang, H., Smith, S. J., Zhang, R., Lou, S., Yu, H., Li, C., and Rasch, P. J.: Source Apportionments of Aerosols
1378 and Their Direct Radiative Forcing and Long-Term Trends Over Continental United States, Earths Future, 6, 793–
1379 808, <https://doi.org/10.1029/2018EF000859>, 2018.

1380 Zender, C., Bian, H., and Newman, D.: Mineral Dust Entrainment and Deposition (DEAD) model: Description and 1990s
1381 dust climatology, J Geophys Res, 108, 4416, doi:10.1029/2002JD002775, 2003.



- 1382 Zhang, Y., Mahowald, N., Scanza, R. A., Journet, E., Desboeufs, K., Albani, S., Kok, J. F., Zhuang, G., Chen, Y., Cohen, D.
1383 D., Paytan, A., Patey, M. D., Achterberg, E. P., Engelbrecht, J. P., and Fomba, K. W.: Modeling the global
1384 emission, transport and deposition of trace elements associated with mineral dust, *Biogeosciences*, 12,
1385 <https://doi.org/10.5194/bg-12-5771-2015>, 2015.
- 1386 Zhao, A., Ryder, C. L., and Wilcox, L. J.: How well do the CMIP6 models simulate dust aerosols?, *Atmos Chem Phys*, 22,
1387 2095–2119, <https://doi.org/10.5194/acp-22-2095-2022>, 2022.
- 1388 Zhao, X., Liu, X., Burrows, S. M., and Shi, Y.: Effects of marine organic aerosols as sources of immersion-mode ice-
1389 nucleating particles on high-latitude mixed-phase clouds, *Atmos Chem Phys*, 21, 2305–2327,
1390 <https://doi.org/10.5194/acp-21-2305-2021>, 2021.
- 1391 Zihan, Q. and Losno, R.: Chemical properties of continental aerosol transported over the Southern Ocean: Patagonian and
1392 Namibian sources, Paris, France, 215 pp., 2016.
- 1393
- 1394



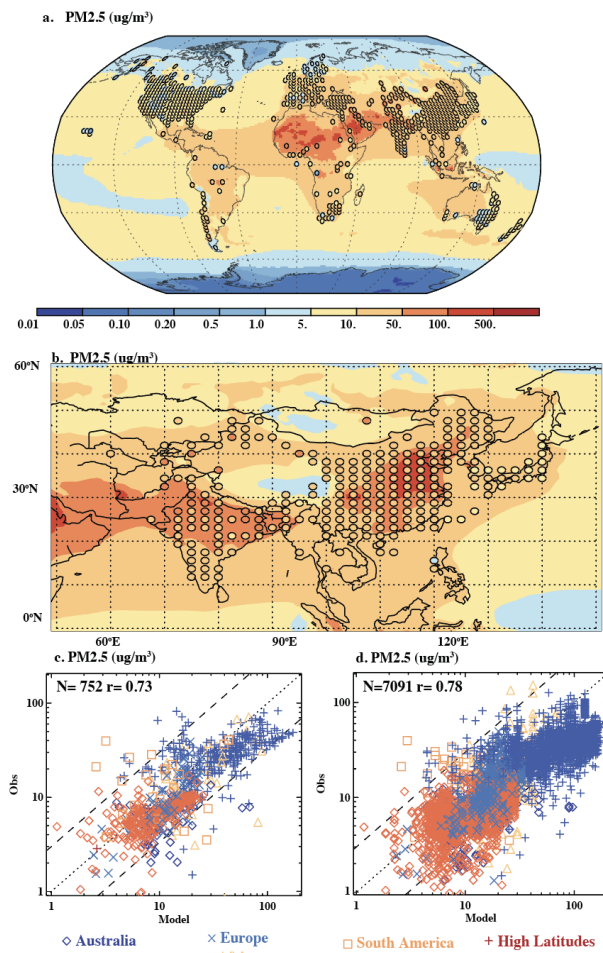
1395

1396 **Figure 1:** Distribution of observations in the data base, showing the number of observations of PM_{2.5} (a) and
1397 PM₁₀ organic carbon (OC) (b) (with the colors indicating different numbers using the top color bar), as well as
1398 the number of stations within each 2x2 grid locations for PM_{2.5} (c) and PM₁₀ OC (d) (using the second color bar),
1399 showing that there is much more PM_{2.5} or PM₁₀ data, in contrast to speciated data. e) The number of observations
1400 (bars) for total particulate matter (PM) or speciated data is summarized for the PM_{2.5} (blue) and PM₁₀ (orange)
1401 fraction using the left-hand side y-axis. The number of stations included in the study is shown as a dotted line (e)



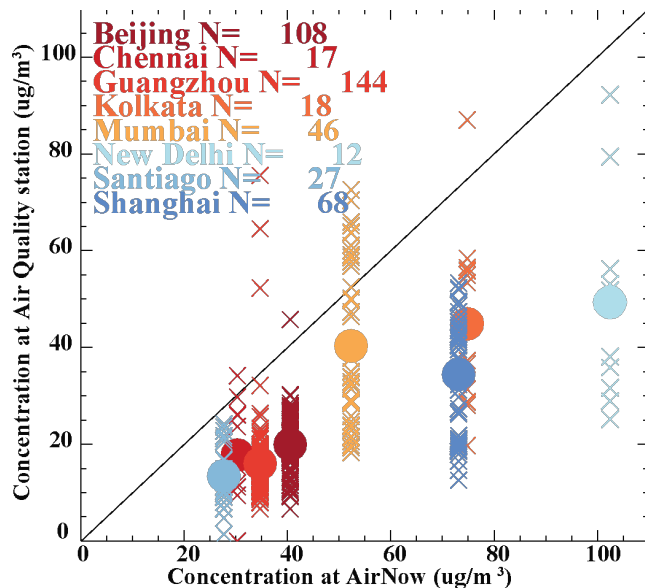
and uses the right-hand size y-axis. f) The number of stations of PM_{2.5} (blue) and PM₁₀ (orange) for each year is shown. g) Normalized (1 standard deviation over the mean) observational uncertainty for PM_{2.5} from measurement errors, interannual variability, measurement method, within grid variability and within year variability at the same station. Interannual variability and within grid uncertainty are defined as the normalized standard deviation in the variability for stations that have more than 10 years of data. Within grid variability is the normalized standard deviation of 2x2 grid cells that have more than 10 stations. Measurement errors are the normalized standard deviation of the reported measurement errors for PM_{2.5}. Measurement method error derives from differences between different measurement methods (e.g., Prank et al., 2016; Burgos et al., 2020; Hand et al., 2017). The stations included derive from the following sources (see supplemental dataset for more details): Alastuey et al., 2016; Almeida et al., 2005; Amato et al., 2016; Andreae et al., 2002; Arimoto et al., 2003; Artaxo et al., 2002; Barkley et al., 2019; Barraza et al., 2017; Bergametti et al., 1989; Bouet et al., 2019; Bozlaker et al., 2013; Chen et al., 2006; Chuang et al., 2005; Cipoli et al., 2023; Cohen et al., 2004; da Silva et al., 2008; Dongarrà et al., 2007, 2010; Engelbrecht et al., 2009; Formenti et al., 2003; Fuzzi et al., 2007; Hand et al., 2017; Heimbürger et al., 2012; Herut and Krom, 1996; Herut et al., 2001; Hsu et al., 2016; Hueglin et al., 2005; Furu et al., 2022, 2015; Gianini et al., 2012a, b; Kalivitis et al., 2007; Kaly et al., 2015; Kubilay et al., 2000; Kyllonen et al., 2020; Laing et al., 2014b, a; Lucarelli et al., 2014, 2019; Mackey et al., 2013; Maenhaut et al., 1996c, a, b, 1997a, b, 1999, 2000a, 2000b, 2002a, b, 2005, 2008, 2011; Maenhaut and Cafmeyer, 1998; Malm et al., 2007; Marticorena et al., 2010; Mihalopoulos et al., 1997; Mirante et al., 2010, 2013; Mkoma, 2008; Mkoma et al., 2009; Morera-Gómez et al., 2018, 2019; Nava et al., 2015, 2020; Nyanganyura et al., 2007; Oliveira, 2009; Oliveira et al., 2010; Pérez et al., 2008; Pio et al., 2022; Prospero et al., 1989, 2012, 2020; Prospero, 1996, 1999; Putaud et al., 2004, 2010; Rodríguez et al., 2011, 2015; Salma et al., 1997; Savoie et al., 1993; Silva et al., 2010; Smichowski et al., 2004; Swap et al., 1992; Tørseth et al., 2012; Uematsu et al., 1983; Vanderzalm et al., 2003; Virkkula et al., 1999; Xiao et al., 2014; Zihan and Losno, 2016. Data from several online networks are also included (e.g., <https://www.airnow.gov/international/us-embassies-and-consulates/>, <https://quotsoft.net/air/>, <https://app.cpcbccr.com/ccr/#/caaqm-dashboard-all/caaqm-landing/data>, <https://sinca.mma.gob.cl/index.php/>, <https://tenbou.nies.go.jp/download/>). See the supplemental data set for more details and the doi links for the datasets.

1429



1430

1431 **Figure 2:** Model results and gridded observations for $\text{PM}_{2.5}$ in $\mu\text{g}/\text{m}^3$ spatially mapped globally (a) and
1432 focused on just East Asia (b) where the model is plotted as the background and the observations are circles with
1433 the colors indicating the amount of $\text{PM}_{2.5}$ using the same scale. A comparison of the model (x-axis) to the
1434 observations (y-axis) is shown for the gridded data (c) and including all stations (d). In the scatter plots, the
1435 colors and symbols indicate the regions, the dotted line is the 1:1 line and the dashed lines are the factor of 3
1436 uncertainty estimates. More statistics are shown in Table S4, and the model plotted alone is available in Figure
1437 S2.
1438



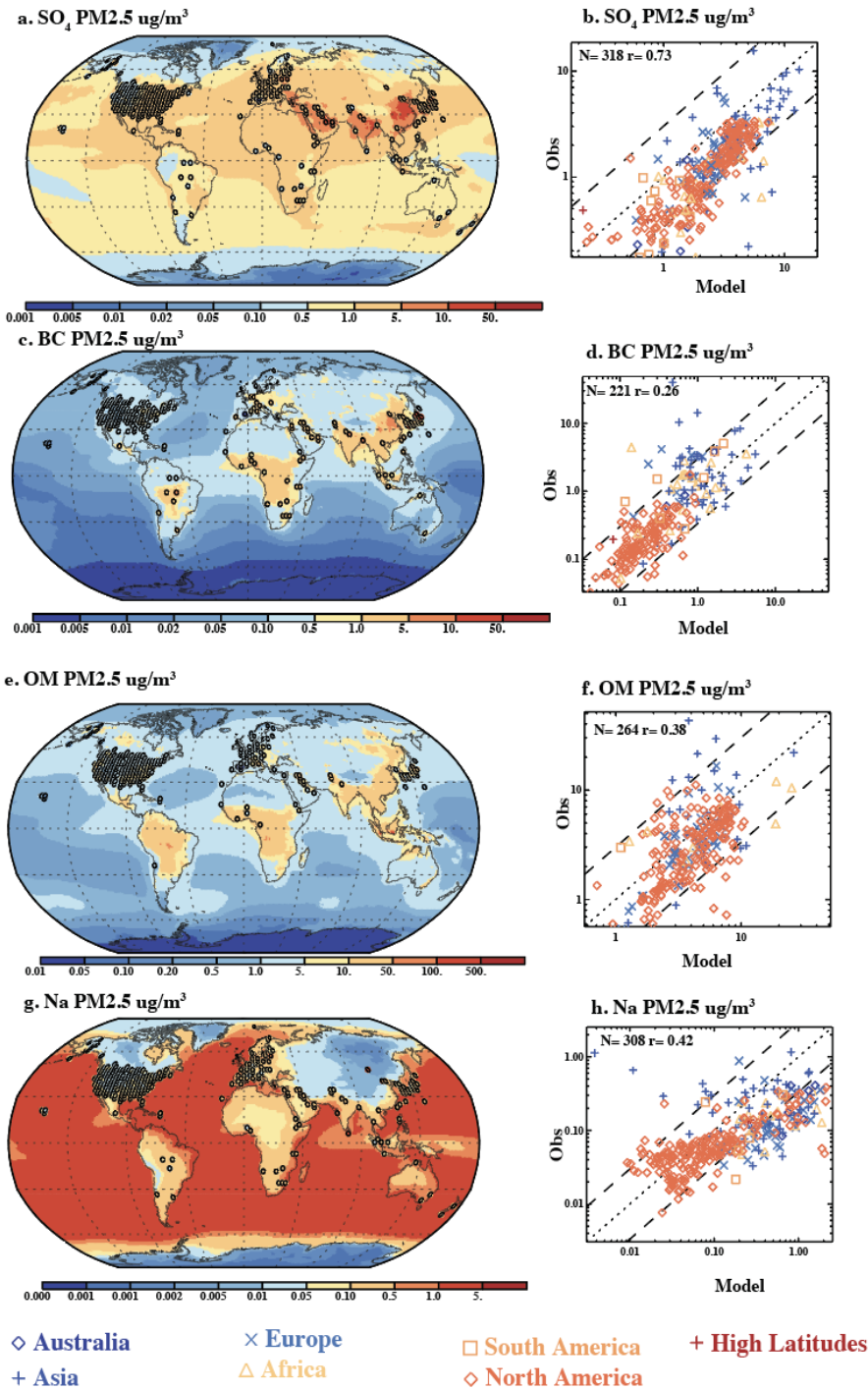
1439

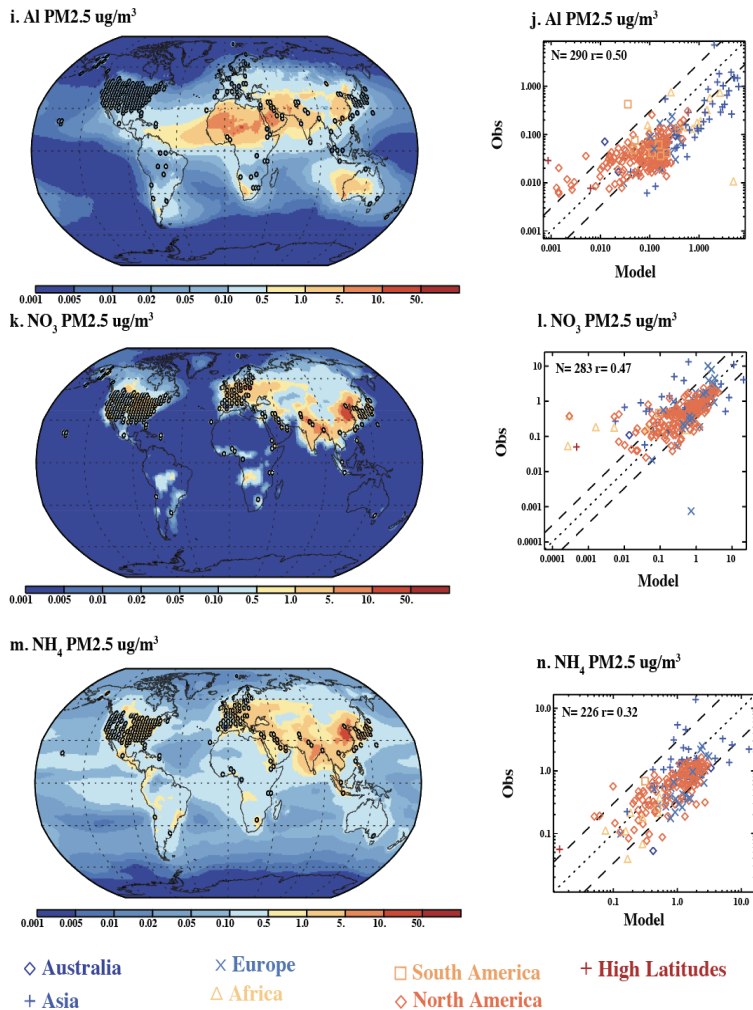
1440 **Figure 3:** Comparison of PM_{2.5} observations from the US Embassy's AirNow network
1441 (<https://www.airnow.gov/international/us-embassies-and-consulates/>) versus observations from the Chinese
1442 air quality network (downloaded from <https://quotsoft.net/air/>) (Beijing 39.9N 116.4E, Guangzhou 23N 113E,
1443 Shanghai 31N 121E) and the Indian (Chennai 13N 80E, Kolkata 23N 88E, New Delhi 27N 77E) network
1444 (<https://app.cpcbccr.com/CCR/#/CAAQM-Dashboard-all/CAAQM-Landing/Data>); and observations (Barraza et al.,
1445 2017) from Santiago, Chile (23.7S 70.4W) against the Chilean air quality network
1446 (<https://sinca.mma.gob.cl/index.php/>). The numbers after each city name are the number of stations found within
1447 1° distance of the AirNow (or Chile observations) station.

1448

1449

1450

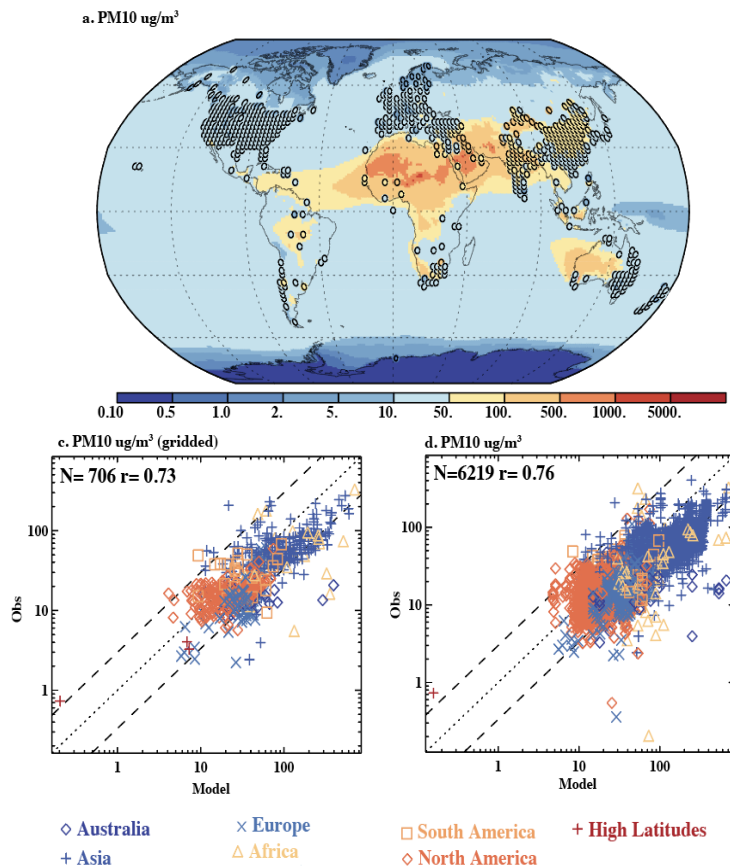




1452

1453 **Figure 4:** Model results and gridded observations for different types of PM_{2.5} in $\mu\text{g}/\text{m}^3$ spatially mapped globally
1454 where the model is plotted as the background and the observations are circles with the colors indicating the
1455 amount PM_{2.5} using the same scale for (a) SO₄²⁻, (c) BC (black carbon), (e) OM (organic material=1.8 times
1456 organic carbon (OC)), (g) Na, (i) Al, (k) NO₃⁻, (m) NH₄⁺. A scatter plot comparison of the model (x-axis) to the
1457 observations (y-axis) is shown for the gridded observational data for for (b) SO₄²⁻, (d) BC (f) OM, (h) Na, (j) Al,
1458 (l) NO₃⁻, (n) NH₄⁺. In the scatter plots, the colors and symbols indicate the regions, the dotted line is the 1:1 line
1459 and the dashed lines are the factor of 3 uncertainty estimates. More statistics are shown in Table S4, and the
1460 model plotted alone is available in Figure S2.

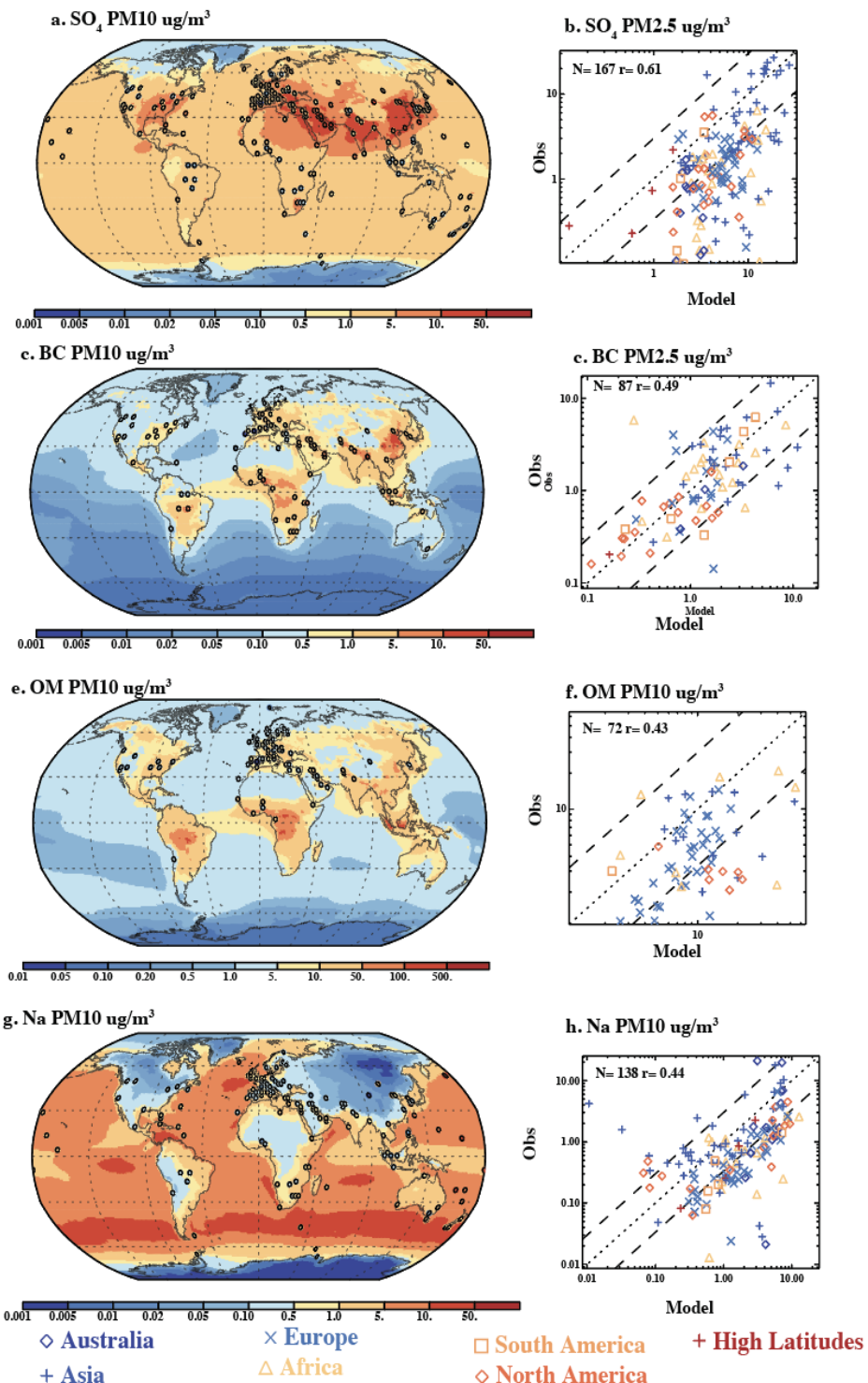
1461

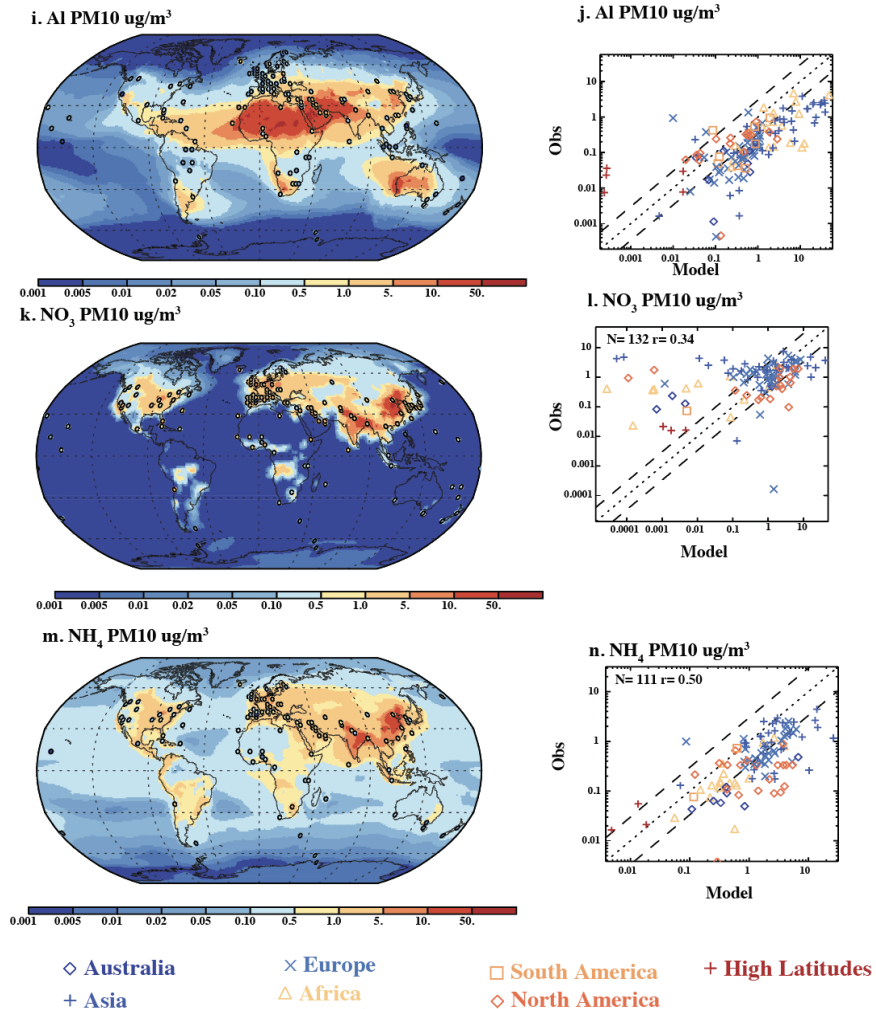


1462

1463 **Figure 5:** Model results and gridded observations for PM₁₀ in $\mu\text{g}/\text{m}^3$ spatially mapped globally (a). A comparison
1464 of the model (x-axis) to the observations (y-axis) is shown for the gridded data (b) and including all stations (c). In
1465 the scatter plots, the colors and symbols indicate the regions, the dotted line is the 1:1 line and dashed lines are
1466 the factor of 3 uncertainty estimates. More statistics are shown in Table S5, and the model plotted alone is
1467 available in Figure S3.

1468





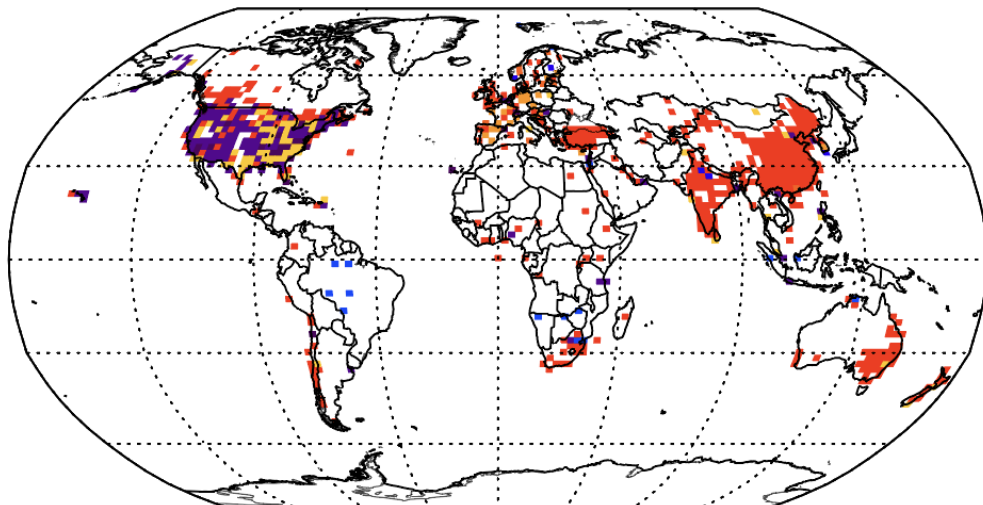
1470

1471 **Figure 6:** Model results and gridded observations for different types of PM₁₀ in $\mu\text{g}/\text{m}^3$ spatially mapped globally
1472 where the model is plotted as the background and the observations are circles with the colors indicating the
1473 amount PM₁₀ using the same scale for (a) SO₄²⁻, (c) BC (black carbon), (e) OM (organic material=1.8 times
1474 organic carbon (OC)), (g) Na, (i) Al, (k) NO₃⁻, (m) NH₄⁺. A scatter plot comparison of the model (x-axis) to the
1475 observations (y-axis) is shown for the gridded observational data for (b) SO₄²⁻, (d) BC (f) OM, (h) Na, (j) Al, (l)
1476 NO₃⁻, (n) NH₄⁺. In the scatter plots, the colors and symbols indicate the regions, the dotted line is the 1:1 line and
1477 the dashed lines are the factor of 3 uncertainty estimates. More statistics are shown in Table S5, and the model
1478 plotted alone is available in Figure S3.

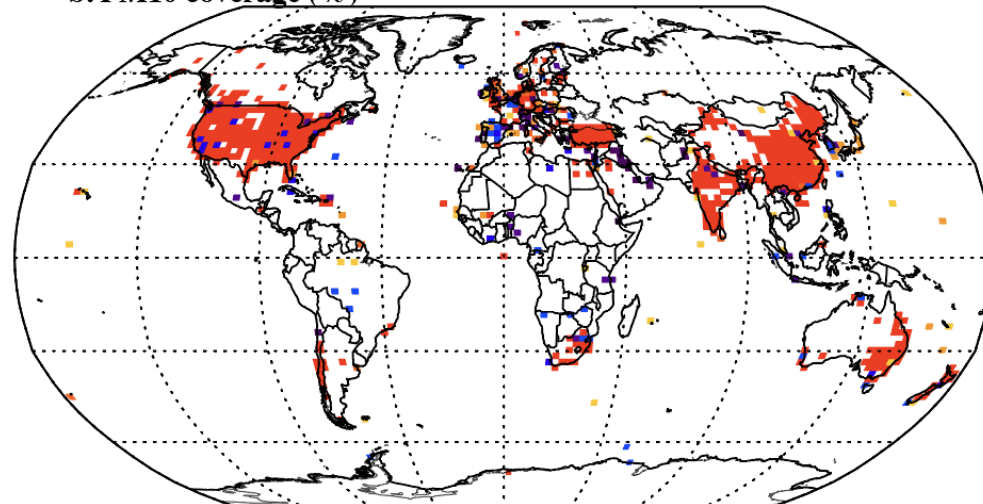
1479



a. PM_{2.5} coverage (%)



b. PM₁₀ coverage (%)



Figure

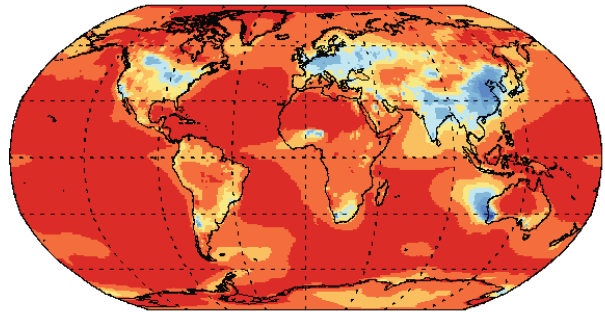
1480

1481 7: Observational coverage (%) for gridded observations, showing within each grid box (2x2) the % of the
1482 constituents that are measured assuming that PM, SO₄²⁻, BC, OM, Na, Al, NO₃⁻, and NH₄⁺ are required to
1483 constrain the PM distribution for (a) PM_{2.5} and (b) PM₁₀.

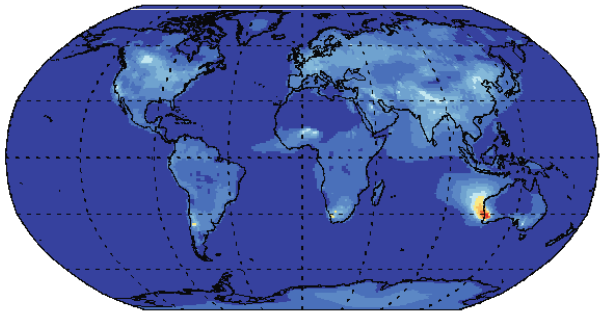
1484



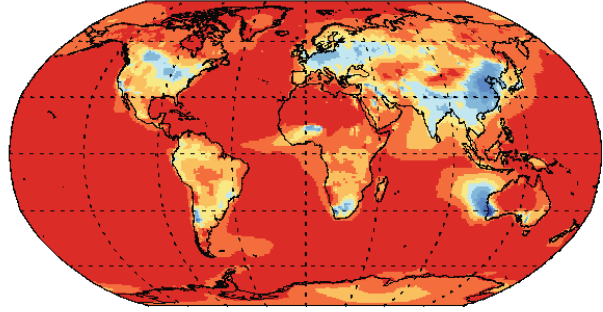
a. PM_{2.5} concentration default sources (%)



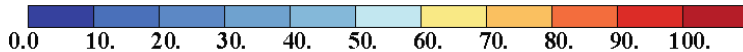
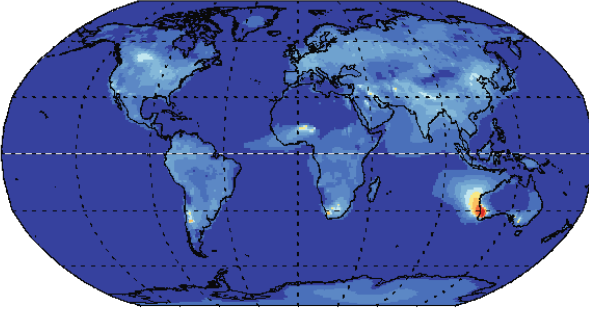
b. PM_{2.5} concentration new sources (%)



c. PM₁₀ concentration default sources (%)



d. PM₁₀ concentration new sources (%)



Figure

8: Modelled estimates of what percent of the surface concentration of PM_{2.5} is considered in the default CAM (a) or is new in this study (b). Similarly PM₁₀ is shown for the default model (c) and new sources in this study (d).

1485

1486

1487

1488

1489

1490



1491 Table 1: Global Aerosol Budgets

1492 Global deposition (Tg/year), percentage of aerosol that is PM_{2.5}, and globally and annually averaged surface concentration
1493 ($\mu\text{g}/\text{m}^3$) and aerosol optical depth for each of the sources used in the model. An asterisk indicates that there are additions to
1494 the model from the default CAM6.

	PM ₁₀	PM _{2.5}		
	Deposition (Tg/year)	%	Conc ($\mu\text{g}/\text{m}^3$)	AOD (unitless)
Sulfate	121	100	2.1	0.018
Black carbon	10	100	0.5	0.009
Primary organic aerosol	34	100	1.6	0.008
Secondary organic aerosol	37	100	1.0	0.007
Sea salts	2520	3	13.0	0.045
Dust	2870	1	19.4	0.030
NH ₄ NO ₃ *	20	100	0.4	0.013
Agricultural Dust*	585	1	3.7	0.006
Road*	0.43	79	0.02	0.0000
Coarse organic carbon*	4	0.0	0.04	0.0000
Coarse black carbon*	0.35	0.0	0.00	0.0000
Fine and coarse inorganic industrial matter *	56	46	1.2	0.0018



Bacteria and Fungi spores from land*	4	0	0.04	0.0000
Other primary biogenic particles from land*	54	3	0.4	0.0005
Marine organic aerosols	44	99	0.6	0.0008

1495

1496

1497